

D7-Brane Motion from M-Theory Cycles and Obstructions in the Weak Coupling Limit

A. P. Braun^a, A. Hebecker^a and H. Triendl^b

^a *Institut für Theoretische Physik, Universität Heidelberg, Philosophenweg 16 und 19
D-69120 Heidelberg, Germany*

^b *II. Institut für Theoretische Physik der Universität Hamburg
Luruper Chaussee 149, D-22761 Hamburg, Germany.*

(a.braun@thphys.uni-heidelberg.de, a.hebecker@thphys.uni-heidelberg.de,
and hagen.triendl@desy.de)

Abstract

Motivated by the desire to do proper model building with D7-branes and fluxes, we study the motion of D7-branes on a Calabi-Yau orientifold from the perspective of F-theory. We consider this approach promising since, by working effectively with an elliptically fibred M-theory compactification, the explicit positioning of D7-branes by (M-theory) fluxes is straightforward. The locations of D7-branes are encoded in the periods of certain M-theory cycles, which allows for a very explicit understanding of the moduli space of D7-brane motion. The picture of moving D7-branes on a fixed underlying space relies on negligible backreaction, which can be ensured in Sen's weak coupling limit. However, even in this limit we find certain 'physics obstructions' which reduce the freedom of the D7-brane motion as compared to the motion of holomorphic submanifolds in the orientifold background. These obstructions originate in the intersections of D7-branes and O7-planes, where the type IIB coupling cannot remain weak. We illustrate this effect for D7-brane models on $\mathbb{CP}^1 \times \mathbb{CP}^1$ (the Bianchi-Sagnotti-Gimon-Polchinski model) and on \mathbb{CP}^2 . Furthermore, in the simple example of 16 D7-branes and 4 O7-planes on \mathbb{CP}^1 (F-theory on K3), we obtain a completely explicit parameterization of the moduli space in terms of periods of integral M-theory cycles. In the weak coupling limit, D7-brane motion factorizes from the geometric deformations of the base space.

1 Introduction

During the last years, significant progress has been made in the understanding of string-theoretic inflation, moduli stabilization, supersymmetry breaking and the fine tuning of the cosmological constant using the flux discretuum. The most studied and arguably best understood setting in this context is that of type IIB orientifolds with D3- and D7-branes [1] (which has close cousins in M-theory [2–4]). Given this situation, it is clearly desirable to develop the tools for particle-phenomenology-oriented model building in this context. One obvious path leading in this direction is the study of the motion of D7-branes in the compact space and their stabilization by fluxes [5–9]. The long-term goal must be to achieve sufficient control of D7-brane stabilization to allow for the engineering of the desired gauge groups and matter content based on the D7-brane open string sector [10]. This is a non-trivial task since the underlying Calabi-Yau geometry has to be sufficiently complicated to allow for the necessary enormous fine tuning of the cosmological constant mentioned above.

In the present paper we report a modest step towards this goal in the simple setting of the 8-dimensional Vafa model, where 16 D7-branes move on T^2/Z_2 [11]. This motion can be viewed equivalently as the deformation of the complex structure of the dual F-theory compactification on K3. The relevant moduli space of D7-brane motion has recently been studied as part of the moduli space of K3×K3 compactifications of F-theory to 4 dimensions (see, e.g. [5, 6, 12]).

One of our main results is the parameterization of the D7-brane motion on the compact space in terms of periods which are explicitly defined using the standard integral homology basis of K3. In other words, we explicitly understand the motion of the 16 D7-branes and of the background geometry in terms of shrinking or growing M-theory cycles stretched between the branes or between the branes and the orientifold planes. In our opinion, this is a crucial preliminary step if one wishes to stabilize specific D7-brane configurations using fluxes (which, in this context, are inherited from M-theory fluxes and depend on the integral homology of K3). Further important points which we discuss in some detail in the following include the geometric implications of Sen’s weak coupling limit [13], the issue of obstructions arising when D7-brane motion is viewed from the type IIB (rather than F-theory) perspective, and the relevance of Sen’s construction of the double-cover Calabi-Yau [13] to type IIB models with branes at singularities [14, 15].

Since the subsequent analysis is necessarily rather technical, we now give a detailed discussion of the organization of the paper, stating the main methods and results of each section.

In Sect. 2, we begin with a discussion of the possible backreaction of D7-branes on the embedding space. This is of immediate concern to us since, in contrast to other D-branes, D7-branes have co-dimension 2 and can therefore potentially modify the surrounding geometry significantly, even in the large volume limit [16–18]. However, following the analysis of [13], it is possible to consider only configurations where $\text{Im } \tau \gg 1$ almost everywhere (weak coupling limit). It is easy to show that, in such a setting, the deficit angle of each brane always remains small ($\sim 1/(\text{Im } \tau)$), while each O-plane has deficit angle π . The solutions that contain a single D7-brane only develop a deficit angle at large distances away from the brane [16–18]. Sen’s weak coupling limit assumes a compact space with proper charge cancellation between D-branes and O-planes, which allows for

the possibility that no deficit angle arises. One may say that, in contrast to other models with branes on Calabi-Yau space, the D7-brane case is special in that one has to take the weak coupling limit more seriously than the large volume limit to be able to neglect backreaction.

In Sect. 3 we discuss obstructions to D7-brane motion. For this purpose, we have to go beyond our simple model with base space \mathbb{CP}^1 . Using the Weierstrass description of an elliptic fibration over \mathbb{CP}^2 or over $\mathbb{CP}^1 \times \mathbb{CP}^1$ (which corresponds to the Bianchi-Sagnotti-Gimon-Polchinski model [19, 20]), it is easy to count the degrees of freedom of D7-brane motion. We find that the motion of D7-branes is strongly restricted as compared to the general motion of holomorphic submanifolds analysed in [7, 21–23]. One intuitive way of understanding these ‘physics obstructions’ is via the realization that D7-branes always have to intersect the O7-plane in pairs or to be tangent to it at the intersection point. We emphasize this issue since it serves as an important extra motivation for our approach via M-theory cycles: If the moduli space is described from the perspective of the M-theory complex structure, such obstructions are automatically included and no extra constraints on the possible motion of holomorphic submanifolds need to be imposed.

Section 4 is devoted to a brief review of the geometry of K3. This is central to our analysis as the moduli space of D7-branes on T^2/Z_2 (or, equivalently, the motion of 16 D7-branes and 4 O7-planes on \mathbb{CP}^1) is dual to the moduli space of M-theory on K3 in the limit where the K3 is elliptically fibred and the volume of the fibre torus is sent to zero. In this language, the weak coupling limit corresponds to sending the complex structure of the torus, which is equivalent to the type IIB axiodilaton τ , to $i\infty$. We recall that the relevant geometric freedom is encoded entirely in the complex structure of K3, which is characterized by the motion of the plane spanned by $\text{Re } \Omega$ and $\text{Im } \Omega$ in a 20-dimensional subspace of $H_2(K3, \mathbb{R})$. Alternatively, the same information can be encoded in two homogeneous polynomials defining a Weierstrass model and thus an elliptic fibration.

In Sect. 5, we recall that at the positions of D7-branes the torus fibre degenerates while the total space remains non-singular. When two or more D7-branes coincide, a singularity of the total space develops, the analysis of which allows for a purely geometric characterization of the resulting ADE gauge symmetry. For the simple case of two merging branes, we show explicitly that a homologically non-trivial cycle of K3 with the topology of a 2-sphere collapses [24, 25]. This collapsing cycle is the basic building block which will allow us to parameterize the full moduli space of D7-brane motion in terms of the periods of such cycles in the remainder of the paper.

In Sect. 6, we start developing the geometric picture of the D7-brane moduli space, which is one of our main objectives in the present paper. Our basic building block is the S^2 cycle stretched between two D7-branes introduced in the previous section. Here, we construct this cycle from a somewhat different perspective: We draw a figure-8-shaped 1-cycle in the base encircling the two branes and supplement it, at every point, with a 1-cycle in the torus fibre. In this picture, it is easy to calculate the intersection numbers of such cycles connecting different D-brane pairs, taking into account also the presence of O-planes (see the figures in this section). The Dynkin diagrams of the gauge groups emerging when several branes coincide are directly visible in this geometric approach. In particular, the relative motion of four branes ‘belonging’ to one of the O-plane can be fully described in terms of the above 2-brane cycles. The pattern of the corresponding

2-cycles translates directly in the Dynkin diagram of $\text{SO}(8)$. To obtain a global picture, we will have to supplement the cycles of these four $\text{SO}(8)$ blocks by further cycles which are capable of describing the relative position of these blocks.

Before doing so we recall, in Sect. 7, the duality of F-theory on K3 to the $\text{E}_8 \times \text{E}_8$ heterotic string on T^2 . This is necessary since we want to relate the geometrically constructed 2-cycles discussed above to the standard integral homology basis of K3, which is directly linked to the root lattice of $\text{E}_8 \times \text{E}_8$. In particular, we explicitly identify the part of the holomorphic 2-form Ω which corresponds to the two Wilson lines of the heterotic theory on T^2 and thus determines the gauge symmetry at a given point in moduli space.

In Sect. 8, we start with the specific form of Ω which realizes the breaking of $\text{E}_8 \times \text{E}_8$ to $\text{SO}(8)^4$ (corresponding to the choice of the two appropriate Wilson lines). The 2-cycles orthogonal to this particular Ω -plane generate the root lattice of $\text{SO}(8)^4$ and can be identified explicitly with our previous geometrically constructed 2-cycles of the four $\text{SO}(8)$ blocks. Thus, we are now able to express these 2-cycles in terms of the standard integral homology basis of K3. Geometrically, this situation corresponds to a base space with the shape of a pillowcase (i.e. T^2/Z_2) with one O-plane and four D-branes at each corner. The remaining four 2-cycles of K3, which are not shrunk, can be visualized by drawing two independent 1-cycles on this pillowcase and multiplying each of them with the two independent 1-cycles of the fibre torus. Thus, we are left with the task of identifying these geometrically defined cycles in terms of the standard homology basis of K3. The relevant space is defined as the orthogonal complement of the space of the $\text{SO}(8)^4$ cycles which we have already identified. We achieve our goal in two steps: First, we consider the smaller (3-dimensional) subspace orthogonal to all $\text{SO}(16)^2$ cycles (their shrinking corresponds to moving all D-branes onto two O-planes and leaving the two remaining O-planes ‘naked’). Second, we work out the intersection numbers with the S^2 -shaped 2-cycles connecting D-branes from different $\text{SO}(8)$ blocks. After taking these constraints into account, we are able to express the intuitive four cycles of the pillowcase in terms of the standard K3 homology basis.

Finally, in Sect. 9, we harvest the results of our previous analysis by writing down a conveniently parameterized generic holomorphic 2-form Ω and interpreting its 18 independent periods explicitly as the 16 D-brane positions, the shape of the pillowcase, and the shape of the fibre torus. Of course, the existence of such a parameterization of the moduli space of the type IIB superstring on T^2/Z_2 is fairly obvious and has been used, e.g., in [5] and in the more detailed analysis of [6]. Our new point is the explicit mapping between the periods and certain geometrically intuitive 2-cycles and, furthermore, the mapping between those 2-cycles and the standard integral homology basis of K3. We believe that this will be crucial for the future study of brane stabilization by fluxes (since those are quantized in terms of the corresponding integral cohomology) and for the generalization to higher-dimensional situations.

We end with a brief section describing our conclusions and perspectives on future work.

2 Deficit angle of D7-branes

In this section we discuss the backreaction of D7-branes on the geometry. In general, Dp -branes carry energy density (they correspond to black-hole solutions for the gravitational background [26]). For $p < 7$, this deforms the geometry at finite distances, but the space remains asymptotically flat at infinity. Thus, backreaction can be avoided by considering D-brane compactifications in the large volume limit.

By contrast, objects with codimension two (such as cosmic strings or D7-branes) produce a deficit angle proportional to their energy density. Thus, a D7-brane in 10 dimensions may in principle have a backreaction on the geometry which is felt at arbitrarily large distances. Let us first consider the effect of the energy density of a D7-brane. From the DBI-action it is easy to see that the gravitational energy density of a D7-brane is proportional to $e^\phi = 1/\text{Im } \tau \equiv 1/\tau_2$. A D7-brane is charged under the axion $C_0 = \text{Re } \tau \equiv \tau_1$, and supersymmetry constrains τ to be a holomorphic function of the coordinates transversal to the D7-brane, see e.g. [18]. As will become apparent in the following, this implies $\tau \rightarrow i\infty$ at the position of the D7-brane. Thus the energy density does not couple to gravity due to the vanishing of the string coupling near the D7-brane.

But there is another effect, first investigated in [16,17], which is due to the coupling of D7-branes to the axiodilaton τ . This coupling produces a non-trivial τ background around their position whose energy deforms the geometry. In flat space this effect produces a deficit angle around the position of the D7-brane at large distance. Let us have a closer look at the case of finite distance and weak coupling, which is important for F-theory constructions in the weak coupling limit.

The relevant part of the type IIB supergravity action is

$$\int d^{10}x \sqrt{g} \left(R + \frac{\partial_\mu \tau \partial_\nu \bar{\tau}}{2\tau_2^2} g^{\mu\nu} \right). \quad (1)$$

The equations of motion (and supersymmetry) imply that τ is a holomorphic function of the coordinate z parameterizing the plane transversal to the brane, $\tau = \tau(z)$. Because of the $SL(2, \mathbb{Z})$ symmetry of IIB string theory acting on τ , it is helpful to use the modular function $j(\tau)$ instead of τ itself for the description of the dependence of τ on z . The function j is a holomorphic bijection from the fundamental domain of $SL(2, \mathbb{Z})$ onto the Riemann sphere and is invariant under $SL(2, \mathbb{Z})$ transformations of τ (details can be found in [27]). Here we need the properties

$$j \sim e^{-2\pi i \tau} \quad \text{for } \tau \rightarrow i\infty, \quad (2)$$

$$j(e^{2\pi i/3}) = 0, \quad (3)$$

$$j(i) = 1. \quad (4)$$

Since τ is holomorphic in z , the modular invariant function $j(\tau)$ depends holomorphically on z , and we can use the Laurent expansion of j in z . As we encircle the D-brane at $z = 0$, j must encircle the origin once in the opposite direction (cf. Eq. (2)). Thus j must be proportional to $1/z$ and we can write

$$j(\tau) \simeq \frac{\lambda}{z} \quad (5)$$

for small z . Here λ is a modulus, the overall scaling of the axiodilaton.

From (1) we also deduce Einstein's equation

$$R_{\mu\nu} = \frac{1}{4\tau_2^2} (\partial_\mu \tau \partial_\nu \bar{\tau} + \partial_\nu \tau \partial_\mu \bar{\tau}) . \quad (6)$$

Note that there is no term representing the energy density of the brane, as argued above. If we parameterize the plane orthogonal to the brane by z and write the metric as

$$ds^2 = \eta_{\mu\nu} dx^\mu dx^\nu + \rho(z, \bar{z}) dz d\bar{z} , \quad (7)$$

we finally arrive at the equation

$$\partial \bar{\partial} \ln \rho = \partial \bar{\partial} \ln \tau_2 , \quad (8)$$

which is solved by $\rho = \tau_2 f(z) \bar{f}(z)$. For the simplest case of a single D7-brane in infinite 10-dimensional space, one might expect that both τ_2 and ρ will not depend on the angle in the complex plane because of radial symmetry. However, this is not the case as we now explain.

The simplest solution is given by declaring Eq. (5) to be exact. Then $\tau(z)$ maps the transverse plane precisely once to the fundamental domain of τ . Remember that the fundamental domain contains three singular points which are fixed points under some $SL(2, \mathbb{Z})$ transformation. These points are

τ	invariant under
$\tau \rightarrow i\infty$	T
$\tau = e^{2\pi i/3}$	ST
$\tau = i$	S ,

where S and T are the standard generators of $SL(2, \mathbb{Z})$. From (2) and (3) we see that the first two of these points are mapped to $|j| \rightarrow \infty$ and $j = 0$. Thus by (5) these points are at the position of the brane and at infinity, respectively. But from (4) we see that the S -monodromy point is somewhere at finite distance and (5) tells us that this point sits at¹ $z = \lambda$. Thus the phase of λ singles out a special direction and the radial symmetry is broken. Nevertheless, if $|\lambda|$ is very large compared to the region we are interested in, there is still an approximate radial symmetry, as can be seen from (2). The monodromy point at $z = \lambda$ does not deform the region near the brane (which is mapped to large τ) and the limit $|\lambda| \rightarrow \infty$ blows up the region where the radial symmetry is preserved. We will see later that this limit corresponds to the weak coupling limit of Sen [13].

We now return to the generic case (where extra branes may be present and (5) is only approximate) and use the assumption that $|\lambda|$ is very large. As we approach a radially symmetric situation in this limit, we can neglect the angular derivatives in (8) and arrive at

$$\frac{1}{r} \frac{\partial}{\partial r} \left(r \frac{\partial \ln \rho}{\partial r} \right) = \frac{1}{r} \frac{\partial}{\partial r} \left(r \frac{\partial \ln \tau_2}{\partial r} \right) , \quad (9)$$

where r is the radius in the (z, \bar{z}) -plane. The deficit angle is given by

$$\alpha = -\pi \cdot r \frac{\partial \ln \rho}{\partial r} . \quad (10)$$

¹This is of course only true approximately if we consider a solution with many branes, so that (5) is the Laurent expansion around the position of a single brane.

Inserting this into (9), we see that

$$\frac{\partial \alpha}{\partial r} = -\pi \cdot \frac{\partial}{\partial r} \left(r \frac{\partial \ln \tau_2}{\partial r} \right) . \quad (11)$$

As discussed before, there is no energy density at the position of the brane and therefore the deficit angle is zero there. By integration we obtain

$$\alpha = -\pi \cdot r \frac{\partial \ln \tau_2}{\partial r} + \pi \cdot r \frac{\partial \ln \tau_2}{\partial r} \Big|_{r=0} . \quad (12)$$

Let us estimate the behavior near the brane, where $\tau \rightarrow i\infty$. From (2) we see that

$$\tau \simeq \frac{i}{2\pi} \ln j \simeq -\frac{i}{2\pi} \ln \frac{z}{\lambda} , \quad (13)$$

and therefore

$$\tau_2 \simeq -\frac{1}{2\pi} \ln \left| \frac{z}{\lambda} \right| . \quad (14)$$

Thus (12) can be evaluated using

$$r \frac{\partial \ln \tau_2}{\partial r} \simeq \frac{\partial \ln(\ln(r/|\lambda|))}{\partial \ln r} = \frac{1}{\ln(r/|\lambda|)} \simeq -\frac{1}{2\pi\tau_2} . \quad (15)$$

Since $\tau_2 \rightarrow \infty$ for $r \rightarrow 0$, the second term in (12) vanishes and we find

$$\alpha \simeq \frac{1}{2\tau_2} . \quad (16)$$

We see that for $r \ll |\lambda|$ this becomes small and therefore, in this limit, the deficit angle is small, too. Thus, we have derived quantitatively at which distances backreaction is small in the weak coupling limit.

Away from the D7-brane the analysis presented above breaks down. This is due to the monodromy point at λ which destroys the radial symmetry of the configuration. To determine the deficit angle that emerges at distances that are much larger than $|\lambda|$, one has to solve (8). The solution, and thus the physics, depends on the boundary conditions that are chosen. These are encoded in the shape of the function $f(z)$, which in turn is determined by the symmetry that is required of the solution. The classic solution of [16,17] which argues for a deficit angle $\pi/6$, demands an $SL(2, \mathbb{Z})$ invariant and non-singular metric. The analysis of [18] argues that, due to its appearance in the definition of the Killing spinor, the function $f(z)$ should be invariant under the monodromy transformations of $\tau(z)$. This requirement introduces another z -dependent factor which leads to an asymptotic deficit angle $2\pi/3$.

Our interpretation of this situation is as follows: In a configuration with a single D7-brane, one has only three monodromy points, T , ST and S in the complex plane. Without loss of generality, we can fix the T -monodromy point (i.e. the D7-brane) at zero and the ST -point at infinity. The definition of a deficit angle, which requires radial symmetry, is possible at distances from the brane much smaller or much larger than that of the S -monodromy point. In the first case the deficit angle is parametrically small, in the second case it is $2\pi/3$ following [18]. Thus, there appears to be no room for a deficit angle $\pi/6$.

3 Sen's Weak Coupling Limit and its Consequences for D7-brane Motion

F-theory is defined by a Weierstrass model on some Kähler manifold [11]. The Weierstrass equation is

$$y^2 = x^3 + fx + g , \quad (17)$$

where f and g are sections of the line bundles $L^{\otimes 4}$ and $L^{\otimes 6}$ respectively. The holomorphic line bundle L is defined by the first Chern class of the base space:

$$c_1(L) = c_1(B) . \quad (18)$$

This equation is derived from the Calabi-Yau condition of F-theory², cf. [13].

The brane positions are given by the zeros of the discriminant of the Weierstrass equation (17)

$$\Delta = 4f^3 + 27g^2 . \quad (19)$$

Before going to the weak coupling limit, these objects are (p, q) branes which cannot be all interpreted as D7 branes simultaneously. Their backreaction on the geometry is strong [11]. Furthermore, the brane motion is constrained because the form of the homogeneous polynomial in (19) is non-generic, i.e., the branes do not move independently.

Let us discuss the weak coupling limit for F-theory compactifications, in which one can formulate everything in terms of D7-branes and O7-planes. Following [13], we parameterize

$$f = C\eta - 3h^2 \quad (20)$$

and

$$g = h(C\eta - 2h^2) + C^2\chi , \quad (21)$$

where C is a constant and η , h and χ are homogeneous polynomials of appropriate degree (i.e. sections of $L^{\otimes n}$). Note that f and g are still in the most general form if we parameterize them as above. The weak coupling limit now corresponds to $C \rightarrow 0$. To see this, consider the modular function j that describes the τ field³:

$$j(\tau) = \frac{4(24f)^3}{4f^3 + 27g^2} = \frac{4(24)^3(C\eta - 3h^2)^3}{\Delta} . \quad (22)$$

The discriminant is given as

$$\Delta = C^2(-9h^2)(\eta^2 + 12h\chi) \quad (23)$$

in the weak coupling limit. We observe that for $C \rightarrow 0$ we have $|j| \rightarrow \infty$ everywhere away from the zeros of h . Locally, this corresponds to the limit $\lambda \rightarrow \infty$ in (5). Furthermore, four pairs of branes merge to form the O-planes at the positions where $h = 0$.

The remaining branes are the D7-branes of this orientifold model. Their position is defined by the equation

$$\eta^2 + 12h\chi = 0 . \quad (24)$$

² From duality to M-theory we know that the compactification manifold of F-theory must be Calabi-Yau in order to preserve $\mathcal{N} = 1$ supersymmetry.

³We have changed the normalization of $j(\tau)$ in order to agree with the physics convention [13].

The left-hand side does not describe the most general section in the line bundle $L^{\otimes 8}$. We conclude that the D7-branes in an orientifold model do not move freely in general. These obstructions have, to our knowledge, so far not been investigated and are not included in the common description of orientifold models. We want to clarify this point further in the following.

As an explicit example we consider the Weierstrass model on $B \equiv \mathbb{CP}^1 \times \mathbb{CP}^1$. The reason why we take this example is that it has already been shown in [28] that the degrees of freedom of the Weierstrass model are in complete agreement with the CFT-description of the T-dual orientifold model, the Bianchi-Sagnotti-Gimon-Polchinski model [19, 20]. By counting the degrees of freedom we will show that this model has less degrees of freedom than a model of freely moving D-branes in the corresponding orientifold model. For this, we take the F-theory model described in [28], go to the weak coupling limit and recombine all O7-planes into a single smooth O7-plane wrapped on the smooth base space of the Weierstrass model. The double-cover Calabi-Yau space is now easily constructed. Furthermore, we recombine all D7-branes into a single smooth D7-brane eliminating all D7-brane intersections. We first assume, following [7] that this D7-brane moves freely as a holomorphic submanifold (respecting, of course, the Z_2 symmetry of the Calabi-Yau). This allows for a straightforward determination of the corresponding number of degrees of freedom from its homology. We will then compare this number with the degrees of freedom that are present in the actual F-theory model.

Let us investigate the F-theory model in greater detail. We call the homogeneous coordinates $[x_1 : x_2]$ for the first \mathbb{CP}^1 , and $[y_1 : y_2]$ for the second \mathbb{CP}^1 . By x and y we denote the generators of the second cohomology, where x corresponds to the cycle that fills out the second \mathbb{CP}^1 and is pointlike in the first \mathbb{CP}^1 , and vice versa for y . In a product of complex projective spaces a section in a holomorphic line bundle corresponds to a homogeneous polynomial. We want to determine the degree of the homogeneous polynomials that will be involved in the calculation. For this purpose, we calculate the first Chern class of the base space:

$$c_1(B) = 2x + 2y . \quad (25)$$

From (18) we conclude that this is the first Chern class of the line bundle L . Thus, sections in L correspond to homogeneous polynomials of degree (2,2) and h , being a section in $L^{\otimes 2}$, is a homogeneous polynomial of degree (4,4). A generic polynomial of degree (4,4) in two complex coordinates is irreducible. Thus, a generic h indeed describes one single O7-plane that wraps both \mathbb{CP}^1 s four times. Similarly, η is a homogeneous polynomial of degree (8,8), and χ is of degree (12,12). The left-hand side of Equation (24) is then a homogeneous polynomial of degree (16,16). This polynomial is generically also irreducible and describes a single D7-brane that wraps both \mathbb{CP}^1 s sixteen times. Note that both h and $\eta^2 + 12h\chi$ do not have any base locus and thus define smooth hypersurfaces in $\mathbb{CP}^1 \times \mathbb{CP}^1$ by Bertini's theorem, cf. [29].

Equation (24) defines an analytic hypersurface S of complex dimension one, which is the position of the D7-brane. This is just a Riemann surface, and in order to identify its topology, it suffices to determine its Euler number. By the methods of [29, 30] it is easy to calculate the Euler number of a hypersurface defined by a homogeneous polynomial. The Euler characteristic is given as

$$\chi(T(S)) = \int_S c_1(T(S)) , \quad (26)$$

The first Chern class of $T(S)$ is given in terms of the Chern classes of the normal bundle of S in B and the tangent bundle of B by the second adjunction formula:

$$c_1(T(S)) = c_1(T(B)) - c_1(N(S)) . \quad (27)$$

The normal bundle of S in B is equivalent to the line bundle that defines S through one of its sections⁴. Putting everything together, we arrive at:

$$\begin{aligned} \chi(T(S)) &= \int_S c_1(T(S)) = \int_S c_1(T(B)) - c_1(N(S)) \\ &= \int_B (c_1(T(B)) - c_1(N(S))) \wedge c_1(N(S)) . \end{aligned} \quad (28)$$

The Chern class of a line bundle on $\mathbb{CP}^1 \times \mathbb{CP}^1$ that has sections which are homogeneous polynomials of degree (n, m) is simply $nx + my$. Together with $c_1(T(\mathbb{CP}^1 \times \mathbb{CP}^1)) = 2x + 2y$ we find that

$$\chi(T(S)) = \int_B ((2 - n)x + (2 - m)y) \wedge (nx + my) = 2(n + m - nm) . \quad (29)$$

Here we used the relations $\int x \wedge y = 1$ and $\int x \wedge x = \int y \wedge y = 0$. By the simple relation $\chi(S) = 2 - 2g$ we can now compute the genus of S , and therefore the Hodge number $h^{(1,0)}(S)$ to be⁵

$$h^{(1,0)}(S) = g = (n - 1)(m - 1) . \quad (30)$$

From [7] we know that the number of holomorphic 1-cycles of a D7-brane in the Calabi-Yau space that are odd under the orientifold action is equal to the number of its valid deformations⁶. Above we computed the number of holomorphic 1-cycles that are even under the orientifold action. To compute the number of holomorphic 1-cycles that are odd under the orientifold projection, we construct the double cover of the brane. The double cover of B is a hypersurface in a \mathbb{CP}^1 -fibration over the base B , which is defined by [13]

$$\xi^2 = h , \quad (31)$$

where ξ is the coordinate in one patch of \mathbb{CP}^1 . This introduces branch points at the location of the O-planes. To get back to the orientifold, one then has to mod out the symmetry $\xi \rightarrow -\xi$. This again gives the orientifold with the topology of B and with O7-planes at the zeros of h .

We thus have to branch S over the intersection points of the O7-plane with the D7-brane. The double cover \tilde{S} of S is then formed by two copies of S that are joined by a number of tubes that is half of the number of intersections. We can compute the number of intersections between the D7-brane and the O7-plane by using the cup product between the corresponding elements in cohomology:

$$I_{(D7,O7)} = \int (4x + 4y) \wedge (nx + my) = 4(n + m) . \quad (32)$$

⁴Note that this means that $c_1(N(S))$ defines a 2-form on B .

⁵One might be worried that setting m or n equal to zero, one can get a surface with $g < 0$. However, a homogeneous polynomial of degree $(n, 0)$ is reducible for $n > 1$, corresponding to a collection of disconnected surfaces.

⁶Note that in [7] this was shown for the case of a Calabi-Yau 3-fold compactification down to four dimensions. Here we consider compactifications on $K3$ down to 6 dimensions. Because the holomorphic n -form then has one leg less, the degree of the relevant cohomology is reduced by one as well.

To compute $h^{(1,0)}$ of \tilde{S} , we simply compute its genus (which is equal to the number of handles of \tilde{S}). Because we are considering the double cover, the genus of \tilde{S} is twice the genus of S , plus a correction coming from intersections between the D7-brane and the O7-plane. As the intersections are pairwise connected by branch cuts which connect S to its image under the orientifold action, they introduce $\frac{1}{2}I_{(D7,O7)} - 1$ extra handles of \tilde{S} . This is illustrated in Fig. 1. Thus $h^{(1,0)}$ of \tilde{S} is given by

$$h^{(1,0)}(\tilde{S}) = g(\tilde{S}) = 2g(S) + \frac{1}{2}I_{(D7,O7)} - 1. \quad (33)$$

Now we can compute the number of holomorphic 1-cycles that are odd under the orientifold projection:

$$h_-^{(1,0)}(\tilde{S}) = h^{(1,0)}(\tilde{S}) - h^{(1,0)}(S) = g(S) + \frac{1}{2}I_{(D7,O7)} - 1 = (n+1)(m+1) - 1. \quad (34)$$

Thus a freely moving D7-brane in an orientifold model, defined by a homogeneous polynomial of degree (n, m) , has $h_-^{(1,0)} = (n+1)(m+1) - 1$ degrees of freedom. This fits nicely with the number of deformations of an arbitrary homogeneous polynomial of degree (n, m) .

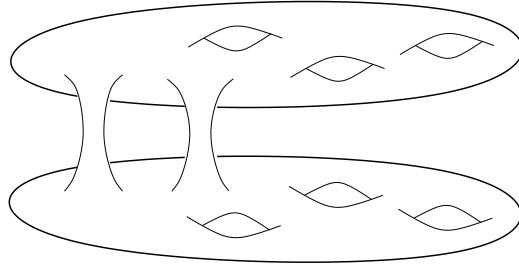


Figure 1: *Illustration of the (double cover of) a D7-brane intersecting an O7-plane in four points.*

Coming back to our example, we see that a freely moving D7-brane on $\mathbb{CP}^1 \times \mathbb{CP}^1$ corresponds to a homogeneous polynomial P of degree $(16, 16)$, giving 288 degrees of freedom. From the F-theory perspective, this polynomial is constrained to be of the form

$$P = \eta^2 + 12h\chi \quad (35)$$

in the weak coupling limit. Here h is fixed by the position of the O-plane. Let us count the degrees of freedom contained in this expression: η is of degree $(8, 8)$, and thus has 81 degrees of freedom. χ is of degree $(12, 12)$ and thus has 169 degrees of freedom. Furthermore, we can always factor out one complex number from this equation so that we have to subtract one degree of freedom. Finally, there is some redundancy that arises through polynomials $K = h^2\alpha^2$ that are both of the form η^2 and $12h\chi$. As α is a polynomial of degree $(4, 4)$, there are 25 redundant degrees of freedom in the present case. Putting everything together, we find that (35) describes 224 degrees of freedom. This differs by 64 degrees of freedom from what we have found for an unconstrained polynomial of degree $(16, 16)$. Note that this is just half of the number of intersections between D7-branes and O7-planes on $\mathbb{CP}^1 \times \mathbb{CP}^1$.

Before discussing the local nature of these ‘physics obstructions’ (which are very different from certain ‘mathematical obstructions’ restricting the motion of holomorphic submanifolds in specific geometries [7, 22, 31, 32]), we want to briefly review a second example. We take the base to be \mathbb{CP}^2 , so that there are 6 O7-planes and 24 D7-branes in the weak coupling limit. We denote the only 2-cycle of \mathbb{CP}^2 , which is a \mathbb{CP}^1 , by x . After recombination we have one D7-brane that wraps the cycle $24x$ and one O7-plane on the cycle $6x$. From $x \cdot x = 1$ we conclude that they intersect 144 times. Now we can repeat counting the degrees of freedom contained in an unconstrained polynomial of degree 24, which is 324, and compare it to a polynomial of the form (35). For \mathbb{CP}^2 , h is of degree 6, χ is of degree 18 and η is of degree 12. By the same arguments as above we find that 252 degrees of freedom are contained in (35) for \mathbb{CP}^2 . The two numbers differ by 72, which is again half of the number of intersections between D7-branes and O7-planes.

It is then natural to expect that the obstructed D7-brane deformations are related to the intersections between D7-branes and O7-planes. Indeed, the smallness of the coupling cannot be maintained in the vicinity of O7-planes. Thus, our argument that the backreaction of D7-branes on the geometry is weak breaks down and we have no right to expect that D7-branes move freely as holomorphic submanifolds at the intersections with O7-planes.

At the level of F-theory, the above physical type-IIB-argument is reflected in the non-generic form of the relevant polynomials in the weak coupling limit. To see this explicitly, let us investigate (35) in the vicinity of an intersection point. We parameterize the neighborhood of this point by complex coordinates z and w . Without loss of generality, we take $h = w$ (i.e. the O7-plane is at $w = 0$) and assume that the intersection is at $z = w = 0$. This means that $P = (\eta^2 + 12h\chi)$ vanishes at $z = w = 0$ and, since we already know that h vanishes at this point, we conclude that $\eta(z = 0, w = 0) = 0$. Expanding η and χ around the intersection point,

$$\eta(z, w) = m_1 z + m_2 w + \dots \quad \text{and} \quad \chi(z, w) = n_0 + n_1 z + n_2 w + \dots ,$$

we find at leading order⁷

$$P = m_1^2 z^2 + 12n_0 w + \dots = 0 . \tag{36}$$

In the generic case $n_0 \neq 0$, this is the complex version of a parabola ‘touching’ the O-plane with its vertex. Thus, we are dealing with a double intersection point.⁸ In the special case $n_0 = 0$, our leading-order P is reducible and we are dealing with two D7-branes intersecting each other and the O7-plane at the same point. The former generic case hence results from the recombination of this D7-D7-brane intersection. In both cases, we have a double intersection point. In other words, the constraint corresponds to the requirement that all intersections between the D7-branes and O7-planes must be double intersection points. There are two easy ways to count the number of degrees of freedom removed by this constraint: On the one hand, demanding pairwise coincidence of the $2n$ intersection points (each of which would account for one complex degree of freedom for a freely moving holomorphic submanifold) removes n degrees of freedom. On the other hand, at each of the n double intersection points the coefficient of the term $\sim z$ in (36) must vanish, which also removes n complex degrees of freedom.

⁷ Note that zw is subdominant w.r.t. to w , which is not true for z^2 .

⁸ This is also clear from the fact that, if we were to introduce by hand a term $\sim z$ in (36), our intersection point would split into two.

To summarize, we have again arrived at the conclusion that $2n$ intersections between a D7-brane and an O7-plane remove n of the degrees of freedom of the D7-brane motion. In particular, we have now shown that these ‘physics obstructions’ have a local reason: In the weak coupling limit, the O7-plane allows only for double intersection points.⁹ At the local level, our findings are easily transferred to compactifications to 4 dimensions: The O7-plane D7-brane intersections are now complex curves rather than points. At each point of such a curve, we can consider the transverse compact space, which is again complex-2-dimensional. In this space, we can perform the same local analysis as above and conclude that double intersection points are required.

We end this section with a comment on an interesting application of F-theory and elliptic fibrations which may be useful for type-IIB model building on the basis of local Calabi-Yau constructions [14, 15]: Consider a non-compact Kähler manifold with $SU(3)$ holonomy (a local Calabi-Yau). Such spaces play an important role in attempts to construct Standard-like models from branes at singularities. We will now sketch a generic procedure allowing us to embed them in a compact Calabi-Yau.

Assuming that the non-compact Kähler manifold is given as a toric variety, it is clearly always possible to make it compact by adding appropriate cones. Furthermore, this can always be done in such a way that the resulting compact Kähler manifold B has a positive first Chern class.¹⁰ With the first Chern class we can associate a line-bundle L and a divisor. Positivity of the Chern class implies that this divisor is effective, i.e., the line bundle L has sections without poles (the zero locus of such a section defines the divisor). Now we can wrap an O7-plane (with four D7-branes on top of it) twice along the above effective divisor. This corresponds to the orientifold limit of a consistent F-theory model. Indeed, as explained at the beginning of this section, we can define a Weierstrass model based on the bundle L on our compact Kähler manifold B . Since $c_1(L) = c_1(B)$, we have constructed an elliptically fibred Calabi-Yau 4-fold and hence a consistent F-theory model. The O7-plane, defined by the zero locus of h , is wrapped twice along the divisor since h is a section of $L^{\otimes 2}$. At this point, we have already realized our local Calabi-Yau as part of a compact type IIB model. It is intuitively clear (although a better mathematical understanding would be desirable) that the O7-plane can be chosen in such a way that it does not interfere with the compact cycles of the original local Calabi-Yau. Indeed, the Calabi-Yau condition has been violated by making the original model compact. This violation is measured by the effective divisor associated with L . This divisor has therefore no need to pass through the region where the original compact cycles (relevant for local Calabi-Yau model building) are localized. We can even go one step further and separate the two O7-planes lying on top of the divisor of L . Subsequently, we can recombine them at possible intersection points, thereby arriving at a single smooth O-plane. Constructing the double cover of the base branched along this O-plane, we obtain a compact Calabi-Yau (without O-plane) the orientifolding of which takes us back to the above F-theory

⁹ This means that some of the 1-cycles that would be present in the double cover of a generic holomorphic submanifold are collapsed in the double cover of a D7-brane in the weak coupling limit. These are the 1-cycles that wind around two branch points.

¹⁰ The fan of a toric Calabi-Yau is spanned by one-dimensional cones that are generated by vectors ending on a single hyperplane H . If we add a one-dimensional cone in the direction opposite to the normal vector n_H of H , we end up with a (in general) non-compact Kähler manifold of positive first Chern class. To make this space compact, we appropriately enlarge the fan. As this can always be done such that all the one-dimensional cones that are added are generated by vectors that end on H , we do not have to change the first Chern class.

model [13]. The compact Calabi-Yau without O-plane constructed in this way contains two copies of the original local Calabi-Yau model.

4 General remarks on $K3$

In two complex dimensions there is, up to diffeomorphisms, just one compact Calabi-Yau manifold: $K3$. We will only collect the facts that we need; for a comprehensive review see e.g. [33].

The Hodge diamond of $K3$ is well known:

$$\begin{array}{ccccc} & & 1 & & \\ & 0 & & 0 & \\ 1 & 20 & & 1. & \\ & 0 & & 0 & \\ & & 1 & & \end{array} \quad (37)$$

The complex structure is measured by the periods z_α which are the integrals of the holomorphic 2-form Ω over integral 2-cycles.

$$z_\alpha \equiv \int_{\gamma_\alpha} \Omega = \int_{K3} \eta_\alpha \wedge \Omega \equiv \eta_\alpha \cdot \Omega . \quad (38)$$

Here η_α are the Poincaré-dual 2-forms corresponding the 2-cycles γ_α . The real Kähler form J can be decomposed in a basis of 2-forms in a similar way. Together, Ω and J specify a point in the moduli space of $K3$. They have to fulfill the constraints

$$\Omega \cdot \Omega = 0 \quad , \quad J \cdot \Omega = 0 \quad , \quad \Omega \cdot \bar{\Omega} > 0 \quad , \quad J \cdot J > 0 . \quad (39)$$

Parameterizing Ω and J by 3 real forms x_i , such that $\Omega = x_1 + i x_2$ and $J \sim x_3$, the constraints translate to

$$x_i \cdot x_j = 0 \quad \text{for} \quad i \neq j \quad (40)$$

and

$$x_1^2 = x_2^2 = x_3^2 > 0 . \quad (41)$$

The symmetry between the three real 2-forms x_i is related to the fact that $K3$ is a hyper-Kähler manifold: there is a whole S^2 of complex structures on $K3$.

The counting of oriented intersection numbers of 2-cycles gives us a symmetric bilinear form on $H_2(K3, \mathbb{Z})$. It can be shown [33] that with this natural scalar product, $H_2(K3, \mathbb{Z})$ is an even self-dual lattice of signature $(3, 19)$. By the classification of even self-dual lattices we know that we may choose a basis for $H_2(K3, \mathbb{Z})$ such that the inner product forms the matrix

$$U \oplus U \oplus U \oplus -E_8 \oplus -E_8 \quad (42)$$

where

$$U = \begin{pmatrix} 0 & 1 \\ 1 & 0 \end{pmatrix} , \quad (43)$$

and E_8 denotes the Cartan matrix of E_8 . Choosing a point in the moduli space of $K3$ is now equivalent to choosing a space-like three-plane in $\mathbb{R}^{3,19}$ equipped with the inner

product (42). This space-like three-plane is spanned by the three vectors x_i fulfilling the conditions (40) and (41)¹¹.

The Picard group, defined as

$$\text{Pic}(X) \equiv H^{1,1}(X) \cap H^2(X, \mathbb{Z}) , \quad (44)$$

is given by the intersection of the lattice $H^2(X, \mathbb{Z})$ with the codimension-two surface orthogonal to the real and imaginary parts of Ω . The dimension of $\text{Pic}(X)$, also called Picard number, counts the number of algebraic curves and vanishes for a generic $K3$ manifold.

If we require $K3$ to admit an elliptic fibration, there are at least two algebraic curves embedded in $K3$ - the T^2 fiber and a section, the latter being equivalent to the base \mathbb{CP}^1 . Thus the space orthogonal to the plane defining the complex structure has a two-dimensional intersection with the lattice $H^2(K3, \mathbb{Z})$, which fixes two complex structure moduli¹². One can show that the two vectors in the lattice corresponding to the base and the fiber form one of the U factors in (42). Thus, Ω has to be orthogonal to the subspace corresponding to this U factor. The precise position of J , which lies completely in this U factor, is fixed by the requirement that the fibre volume goes to zero in the F-theory limit. The only remaining freedom is in the complex structure, which is now defined by a space-like two-plane in $\mathbb{R}^{2,18}$ with the inner product

$$U \oplus U \oplus -E_8 \oplus -E_8 . \quad (45)$$

Any vector in the lattice of integral cycles of an elliptically fibred $K3$ can now be written as

$$D = p^i e^i + p_j e_j + q_I E_I, \quad (46)$$

where i, j run from one to two and I, J from 1 to 16. The p_i as well as the p^i are all integers. The $E_8^{\oplus 2}$ lattice is spanned by q_I fulfilling $\sum_{I=1..8} q_I = 2\mathbb{Z}$, $\sum_{I=9..16} q_I = 2\mathbb{Z}$. In each of the two E_8 blocks, the coefficients furthermore have to be *all* integer or *all* half-integer [34]. The only non-vanishing inner products among the vectors in this expansion are

$$E_I \cdot E_J = -\delta_{IJ} \quad e^i \cdot e_j = \delta_j^i . \quad (47)$$

There are 18 complex structure deformations left in the elliptically fibred case: Ω may be expanded in twenty two-forms, which leads to 20 complex coefficients. However, there is still the possibility of an arbitrary rescaling of Ω by one complex number, as well as the complex constraint $\Omega \cdot \Omega = 0$, so that we find an 18-dimensional complex structure moduli space.

This number can easily be compared to the moduli of $K3$ considered as an elliptic fibration over \mathbb{CP}^1 [11], defined by the Weierstrass equation

$$y^2 = x^3 + f_8(a, b)x + g_{12}(a, b) \quad (48)$$

¹¹ We identify $H_2(K3, \mathbb{R})$ and $H^2(K3, \mathbb{R})$ here and below.

¹² This behavior is a specialty of $K3$ and is related to the fact that, contrary to higher-dimensional Calabi-Yau spaces, $h^{1,1} \neq b^2$.

where $[a : b]$ are the homogeneous coordinates of \mathbb{CP}^1 and f_8 and g_{12} are homogeneous polynomials of degree 8 and 12 respectively. They are determined by $9 + 13 = 22$ parameters. There is an $SL(2, \mathbb{C})$ symmetry acting on the homogeneous coordinates of the base \mathbb{CP}^1 and an overall rescaling of (48). This reduces the independent number of parameters to 18 [11]. From the perspective of F-theory compactified on $K3$, 17 of these 18 parameters describe the locations of D7-branes and O-planes on the base of the fibration, \mathbb{CP}^1 . The remaining parameter describes the complex structure of the fiber and corresponds to the axiodilaton τ . At the same time, these 18 parameters describe the variation of the complex structure of the $K3$, so that one can interpret D-brane moduli as complex structure moduli of an elliptically fibred higher-dimensional space.

5 Singularities and the Weierstrass model.

As D7-branes are characterized by a degeneration of the elliptic fibre one may wonder whether the total space, in our case $K3$, is still smooth. Its defining equation shows that $K3$ is generically smooth and only the fibration becomes singular. If the discriminant of the Weierstrass model has multiple zeros, corresponding to placing multiple branes on top of each other, the total space becomes singular as well. In the case of elliptic $K3$ manifolds, the classification of singularities matches the classification of the appearing gauge groups.

The zeros of the discriminant

$$\Delta = 4f^3 + 27g^2 \quad (49)$$

determine the points of the base where the roots of the Weierstrass equation degenerate. Let us examine this further. The Weierstrass equation (48) can always be written in the form¹³

$$y^2 = (x - x_1)(x - x_2)(x - x_3) . \quad (50)$$

It is easy to show that in this notation

$$\Delta = (x_1 - x_2)^2(x_2 - x_3)^2(x_3 - x_1)^2 . \quad (51)$$

At a point where the fibre degenerates, two of the x_i coincide so that, adjusting the normalization for convenience, (48) reads locally

$$y^2 = (x - x_0)^2 . \quad (52)$$

By a change of variables this is equivalent to $xy = 0$, representing an A_1 singularity of the fibre. To see what happens to the whole space we have to keep the dependence on the base coordinates. Let us deform away from the degenerate point by shifting $x_0 \rightarrow x_{\pm} = x_0 \pm \delta$. This means that now

$$y^2 = (x - x_+)(x - x_-) = (x - x_0)^2 + \delta^2 . \quad (53)$$

The quadratic difference of the now indegenerate roots is given by

$$(x_+ - x_-)^2 = 4\delta^2 . \quad (54)$$

¹³ Note that the term quadratic in x is absent in the canonical form (48). This corresponds to choosing the origin of our coordinate system such that the three roots x_i sum up to zero.

Comparing this with (51) and ignoring the slowly varying factor associated with the distant third root, we have

$$\delta^2 \sim \Delta. \quad (55)$$

Since we also want to see what happens to the full space, we reintroduce the dependence on the base coordinates, $\Delta = \Delta(a, b)$, and write (53) as

$$y^2 = (x - x_0)^2 + \Delta(a, b). \quad (56)$$

Without loss of generality we assume $a \neq 0$ and use a as an inhomogeneous coordinate. Near the singularity, where $\Delta = (a - a_0)^n$, the Weierstrass model then reads

$$y^2 = (x - x_0)^2 + (a - a_0)^n \quad (57)$$

which is clearly singular if n is greater than one. By a change of variables this is again equivalent to

$$yx = (a - a_0)^n. \quad (58)$$

Thus, simple roots ($n = 1$) of Δ do not lead to any singularity of the whole space, it is merely the fibration structure that becomes singular.

We have seen that the $K3$ surface has a singularity when two or more branes are on top of each other, whereas it is smooth when they are apart. If we move the two branes apart by perturbing the polynomials in the Weierstrass equation, we remove the singularity and blow up an exceptional 2-cycle. We will make this explicit in the following. The emerging cycle will subsequently be used to measure the distance between the two branes.

From (57) we see that the situation of two merging branes is described by

$$X \equiv \{x, y, a \mid x^2 + y^2 + a^2 = \epsilon\}. \quad (59)$$

We have shifted x and a for simplicity. Here a is an affine coordinate on the base and ϵ resolves the singularity by moving the two branes away from each other.

As the situation is somewhat analogous to the conifold case [35], we will perform a similar analysis: We first note that ϵ can always be chosen to be real by redefining the coordinates. Next, we collect x, y, a in a complex vector with real part ξ and imaginary part η . The hypersurface (59) may then be described by the two real equations

$$\xi^2 - \eta^2 = \epsilon, \quad \xi \cdot \eta = 0. \quad (60)$$

We can understand the topology of X by considering its intersection with a set of 5-spheres in \mathbb{R}^6 given by $\xi^2 + \eta^2 = t$, $t > \epsilon$:

$$\xi^2 = \frac{t}{2} + \frac{\epsilon}{2}, \quad \eta^2 = \frac{t}{2} - \frac{\epsilon}{2}, \quad \xi \cdot \eta = 0. \quad (61)$$

If we assume for a moment that $\epsilon = 0$, the equations above describe two S^2 s of equal size for every t that are subject to an extra constraint. If we take the first S^2 to be unconstrained, the second and third equation describe the intersection of another S^2 with a hyperplane. Thus we have an S^1 bundle over S^2 for every finite t . This bundle shrinks to zero size when t approaches zero so that we reach the tip of the cone. Furthermore,

the bundle is clearly non-trivial since the hyperplane intersecting the second S^2 rotates as one moves along the first S^2 .

Let us now allow for a non-zero ϵ , so that X is no longer singular. The fibre S^1 still shrinks to zero size at $t = \epsilon$, but the base S^2 remains at a finite size. This is the 2-cycle that emerged when resolving the singularity. We now want to show that the S^2 at the tip of the resolved cone is indeed a non-trivial cycle. This is equivalent to showing that the bundle that is present for $t > \epsilon$ does not have a global section, i.e., the S^2 at $t = \epsilon$ cannot be moved to larger values of t as a whole. Consider a small deformation of this S^2 , parameterized by a real function $f(\xi)$:

$$\xi^2 = \epsilon + f(\xi) . \quad (62)$$

This means that we have moved the S^2 at $t = \epsilon$ in the t -direction by $2f(\xi)$, i.e.

$$\frac{t}{2} = f(\xi) + \frac{\epsilon}{2} . \quad (63)$$

The equations for the S^1 fibration over this deformed S^2 read

$$\eta^2 = f(\xi) \quad (64)$$

$$\eta \cdot \xi = 0 . \quad (65)$$

Deforming the S^2 means choosing a continuous function $\eta(\xi)$ subject to these equations. Since the set of all planes defined by (65) can be viewed as the tangent bundle of an S^2 , we can view $\eta(\xi)$ as a vector field on S^2 . As we know that such vector fields have to vanish in at least two points, we conclude that $f(\xi)$ has to vanish for two values of ξ . We do not only learn that the S^2 at the tip of the cone cannot be moved away, but also that the modulus of its self-intersection number is two¹⁴. This number is expected, as one can show that any cycle of $K3$ with the topology of a sphere has self-intersection number minus two [33].

A similar analysis can be carried out for other types of singularities, which are determined by the orders with which f , g and Δ vanish [36]. For the whole $K3$, we can use the ordinary ADE classification of the arising quotient singularities [33], which is equivalent to the classification of simply laced Lie algebras. The intersection pattern of the cycles that emerge in resolving the singularity is precisely the Dynkin diagram of the corresponding Lie algebra. This ‘accidental’ match is of course expected from the F-theory point of view which tells us that singularities are associated with gauge groups. The correspondence between the singularity type of the whole space and the singularity type of the fibre is more complicated when F-theory is compactified on a manifold with more than two complex dimensions [37–40]. This can also be anticipated from the fact that gauge groups which are not simply laced appear only in IIB orientifolds with more than one complex dimensions.

¹⁴ Note that this viewpoint also works for the classic conifold example [35], which is a cone whose base is an S^2 bundle over S^3 . As the Euler characteristic of S^3 vanishes, the same arguments as before give the well-known result that the S^3 at the tip of the resolved conifold can be entirely moved into the base.

6 Geometric picture of the moduli space

In this section we want to gain a more intuitive understanding of the cycles that are responsible for the brane movement. For this we picture the elliptically fibred K3 locally as the complex plane (in which branes are sitting) to which a torus has been attached at every point. We will construct the relevant 2-cycles geometrically. We have already seen that the cycles in question shrink to zero size when we move the branes on top of each other, so that these cycles should be correlated with the distance between the branes. Remember that D7-branes have a non-trivial monodromy acting on the complex structure of the fibre as $\tau \rightarrow \tau + 1$, which has

$$T = \begin{pmatrix} 1 & 1 \\ 0 & 1 \end{pmatrix} \quad (66)$$

as its corresponding $SL(2, \mathbb{Z})$ matrix. Similarly, O7-planes have a monodromy of $-T^4$, where the minus sign indicates an involution of the torus, meaning that the complex coordinate z of the torus goes to $-z$. Thus 1-cycles in the fibre change orientation when they are moved around an O-plane.

If we want to describe a 2-cycle between two D-branes, it is clear that it must have one leg in the base and one in the fibre to be distinct from the 2-cycles describing the fibre and the base. Now consider the 1-cycle being vertically stretched in the torus¹⁵. If we transport this cycle once around a D-brane and come back to the same point, this cycle becomes diagonally stretched because of the T-monodromy. If we then encircle another brane in the opposite direction, the 1-cycle returns to its original form, so that it can be identified with the original 1-cycle. This way to construct a closed 2-cycle was already mentioned in [24]. This 2-cycle cannot be contracted to a point since it cannot cross the brane positions because of the monodromy in the fibre. The form of the 2-cycle is illustrated in Fig. 2. We emphasize that to get a non-trivial cycle, its part in the fibre torus has to have a vertical component.

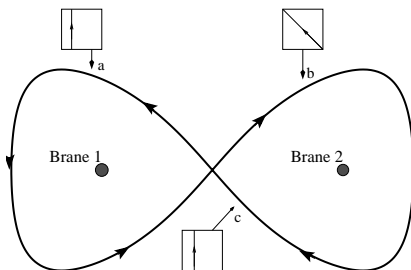


Figure 2: *The cycle that measures the distance between two D-branes. Starting with a cycle in the $(0, 1)$ direction of the fibre torus at point a , this cycle is tilted to $(-1, 1)$ at b . Because we surround the second brane in the opposite way, the cycle in the fibre is untilted again so it can close with the one we started from.*

Next we want to compute the self-intersection number. In order to do this, we consider a homologous cycle and compute the number of intersections with the original one. By

¹⁵Of course this notion depends on the $SL(2, \mathbb{Z})$ -frame we consider, but anyway we construct the cycle in the frame where the branes are D-branes. In the end the constructed cycle will be independent of the choice of frame.

following the way the fibre part of the cycle evolves, one finds that the resulting number is minus two (see Fig. 3). The minus sign arises from the orientation. This is precisely what we expected from the previous analysis. To see the topology of the cycle more clearly, it is useful to combine the two lines in the base stretching between the branes to a single line. This is shown in Fig. 4. The component of the cycle in the fibre is then an S^1 that wraps the fibre in the horizontal direction, so that it shrinks to a point at the brane positions. Thus it is topologically a sphere, which fits with the self-intersection number of -2 and the discussion of the previous section.

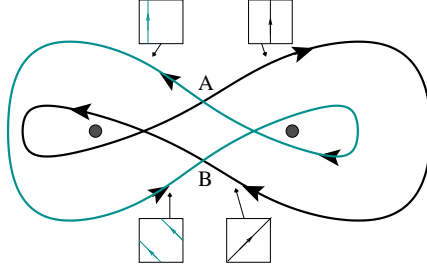


Figure 3: *The self-intersection number of a cycle between two D-branes. As shown in the picture, we may choose the fibre part of both cycles to be $(0, 1)$ at A, so that they do not intersect at this point. At B however, one of the two is tilted to $(1, 1)$, whereas the other has undergone a monodromy transforming it to $(-1, 1)$. Thus the two surfaces meet twice in point B.*

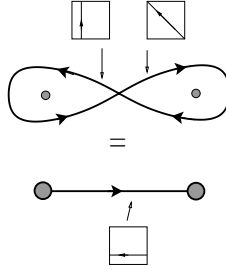


Figure 4: *The loop between two D-branes can be collapsed to a line by pulling it onto the D-branes and annihilating the vertical components in the fibre. All that remains is a cycle which goes from one brane to the other while staying horizontal in the fibre all the time.*

Now we want to determine the intersection number between different cycles and consider a situation with three D7-branes. There is one cycle between the first two branes and one between the second and the third, each having self-intersection number -2 . From Fig. 5 it should be clear that they intersect exactly once. If one now compares the way they intersect to the figure that was used to determine the self-intersection number, one sees that the two surfaces meet with one direction reversed, hence the orientation differs and we see that the mutual intersection number is $+1$. Thus we have shown that the intersection matrix of the $N - 1$ independent cycles between N D-branes is minus the Cartan Matrix of $SU(N)$.

We now want to analyze the cycles that arise in the presence of an O7-plane. Two D7-branes in the vicinity of an O7-plane can be linked by the type of cycle considered above.

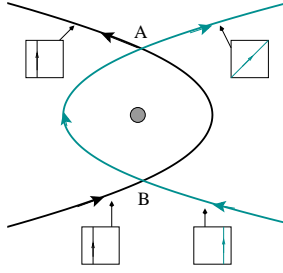


Figure 5: *Mutual intersection of two cycles. Start by taking both cycles to have fibre part $(0,1)$ at B . The fact that we closed a circle around the D-brane tells us that one of the two has been tilted by one unit at A . Thus they meet precisely once.*

However, there are now two ways to connect the D-branes with each other: we can pass the O-plane on two different sides, as shown in Fig. 6. By the same argument as before, each of these cycles has self-intersection number -2 . To get their mutual intersection number, it is important to remember the monodromy of the O-plane, which contains an involution of the torus fiber. Thus, the intersection on the right and the intersection on the left, which differ by a loop around the O-plane, have opposite sign. As a result, the overall intersection number vanishes.

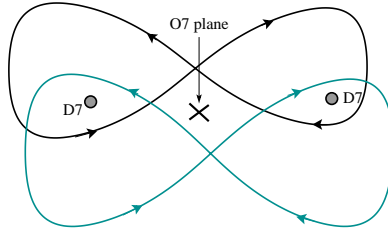


Figure 6: *Cycles that measure how D-branes can be pulled onto O-planes.*

Now we have all the building blocks needed to discuss the gauge enhancement in the orientifold limit, which is $SO(8)^4$. We should find an $SO(8)$ for each O7-plane with four D7-branes on top of it. The cycles that are blown up when the four D7-branes move away from the O7-plane are shown in Fig. 7. It is clear from the previous discussion that all cycles have self-intersection number -2 and cycle c intersects every other cycle precisely once. Thus, collecting the four cycles in a vector (a, b, c, d) , we find the intersection form

$$D_4 = \begin{pmatrix} -2 & 0 & 1 & 0 \\ 0 & -2 & 1 & 0 \\ 1 & 1 & -2 & 1 \\ 0 & 0 & 1 & -2 \end{pmatrix}, \quad (67)$$

which is minus the Cartan matrix of $SO(8)$. It is also easy to see that collapsing only some of the four cycles yields minus the Cartan matrices of the appropriate smaller gauge enhancements.

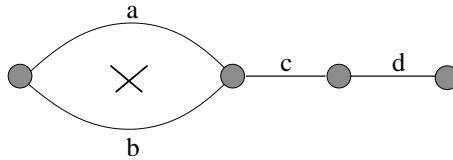


Figure 7: *Four D-branes and an O-plane. The D-branes are displayed as circles and the O-plane as a cross. To simplify the picture we have drawn lines instead of loops.*

7 Duality to M-theory and heterotic $E_8 \times E_8$

In this section we give a brief review of the dualities between F-theory and M-theory, as well as between F-theory and the $E_8 \times E_8$ heterotic string. We focus on the points relevant to the discussion in this paper.

As M-theory compactified on S^1 is dual to type IIA in 10 dimensions, we can relate M-theory to type IIB by compactifying on a further S^1 and applying T-duality. Thus, M-theory on T^2 corresponds to type IIB on S^1 . The complexified type-IIB coupling constant is given by the complex structure of the torus. Furthermore, taking the torus volume to zero corresponds to sending the S^1 radius on the type IIB side to infinity. In other words, M-theory on T^2 with vanishing volume gives type IIB in 10 dimensions. One may think of this as a T^2 compactification of a 12d theory, which we take as our working definition of F-theory. Considering the compactification of M-theory on an elliptically fibred manifold Y and using the above argument for every fibre, we arrive at type IIB on the base space. This can be re-expressed as an F-theory compactification on Y .

One can now study the stabilization of D7-branes through fluxes by investigating the stabilization of a (complex) fourfold Y on the M-theory side and mapping the geometry to the D-brane positions [5, 6]. One can also translate the 4-form fluxes of M-theory to 3- and 2-form fluxes in the IIB picture. In particular, we can consider 4-cycles built from a 2-cycle stretched between two D7-branes (see previous section) and a 2-cycle of the D7-brane. We then expect 2-form flux on D7-branes to arise from M-theory 4-form flux on such cycles. This fits nicely with the fact that 2-form flux on D7-branes T-dualizes to an angle between two intersecting D6-branes, so that it is only defined relative to the flux on another D7-brane. Note that being in the F-theory limit (i.e. ensuring that Y is elliptically fibred and the fiber volume vanishes) also has to be realized by an appropriate flux choice on the M-theory side.

The foundation of the duality between F-theory and the $E_8 \times E_8$ heterotic string is the duality between M-theory compactified on $K3$ and the heterotic string compactified on T^3 [41]. In the limit in which the fibre of $K3$ shrinks (the F-theory limit), one S^1 decompactifies so that we end up with heterotic $E_8 \times E_8$ on T^2 [11, 25, 42–44].

In this duality the complex structure of the base and the fibre of $K3$ are mapped to the complex and Kähler structure moduli of the T^2 on the heterotic side. The precise relation between these parameters has been worked out in [43]. The volume of the base of $K3$ corresponds to the coupling of the heterotic theory. The breaking of $E_8 \times E_8$ that is achieved by Wilson lines on the heterotic side appears in the form of deformations of the Weierstrass equation away from the $E_8 \times E_8$ singularity on the F-theory side. This is equivalent to deforming the complex structure of $K3$.

Let us examine this point in more detail: we can parameterize the complex structure of $K3$ at the $E_8 \times E_8$ point by

$$\Omega_{E_8 \times E_8} = e^1 - \tilde{U}\tilde{S}e_1 + \tilde{U}e^2 + \tilde{S}e_2 . \quad (68)$$

We have set the first coefficient to one by a global rescaling and used the fact that $\Omega \cdot \Omega = 0$. We can now add a component in the direction of the E_8 factors to (68) in order to break the gauge group.

In the heterotic theory, the Wilson lines are two real vectors that are labelled by their direction in T^2 : W_I^1 and W_I^2 . Let us normalize these Wilson lines such that the associated gauge-theoretical twist is

$$P = e^{-2\pi i W_I^1 E_I} , \quad (69)$$

with the action

$$E_\gamma \rightarrow P E_\gamma P^{-1} = e^{-2\pi i \gamma_I W_I^1} E_\gamma , \quad (70)$$

and analogously for W_I^2 . This means that, whenever there is a root vector γ such that $\gamma \cdot W^1$ and $\gamma \cdot W^2$ are integers, the corresponding root survives the Wilson line breaking.

Let us define $W_I E_I = W_I^1 E_I + \tilde{U} W_I^2 E_I$ and write the complex structure at a general point in moduli space as

$$\Omega = e^1 + \tilde{U}e^2 + \tilde{S}e_2 - \left(\tilde{U}\tilde{S} + \frac{1}{2}(W)^2 \right) e_1 + W_I E_I . \quad (71)$$

Here we denote $(W_I^1 E_I + \tilde{U} W_I^2 E_I)^2$ simply by $(W)^2$. Note that $\Omega \cdot \Omega = 0$ holds for all values of the parameters. If we find a surviving root $\gamma = \gamma_I E_I$ in the $E_8 \times E_8$ lattice, its inner product with the complex structure is $\Omega \cdot \gamma = -n - \tilde{U}m$. This means there exists a cycle $\gamma' \equiv \gamma_I E_I + n e_1 + m e_2$ with the property $\Omega \cdot \gamma' = 0$, implying that this cycle has shrunk to zero size. Thus, extra massless states are present and a gauge enhancement arises, which is precisely what one expects from a surviving root on the heterotic side. We can conclude that, by (71), we have consistently identified the properly normalized Wilson lines W^1 and W^2 of the heterotic description with the appropriate degrees of freedom of the complex structure of $K3$ on the F-theory side.

8 The $SO(8)^4$ singularity of $K3$

If we describe the possible deformations of $K3$ by deformations of the defining functions of the Weierstrass model, f and g , we see that singularities arise at specific points in moduli space. We can also describe the deformations of $K3$ as deformations of the complex structure, Ω . In this description we can also reach points in the moduli space where the $K3$ is singular. By comparing the singularities, we can map special values of the complex structure moduli to a special form of the Weierstrass model. This enables us to describe the positions of the D-branes and O-planes, which are explicit in the polynomial description, by the values of the complex structure moduli of $K3$.

In the language of complex structure deformation, the $K3$ becomes singular if we can find a root, i.e. an element of $H^2(\mathbb{Z})$ with self intersection -2 that is orthogonal to both

Ω and J . If we now consider the inner product on the sublattice spanned by such roots, we find minus the Cartan Matrix of some ADE group. This structure tells us the kind of singularity that has emerged [5, 33].

We now want to discuss the cycles that shrink to produce an $SO(8)^4$ singularity. For this we have to find a change of basis such that the $D_4^{\oplus 4}$ in the inner product of the lattice $H^2(K3, \mathbb{Z})$ becomes obvious. The well-known Wilson lines breaking $E_8 \times E_8$ down to $SO(8)^4$ are

$$W^1 = \left(0^4, \frac{1}{2}^4, 0^4, \frac{1}{2}^4\right) \quad W^2 = (1, 0^7, 1, 0^7) . \quad (72)$$

W^2 breaks $E_8 \times E_8$ down to $SO(16) \times SO(16)$, W^1 breaks this further down to $SO(8)^4$. Inserting this in (71), we find Ω at the $SO(8)^4$ point:

$$\Omega_{SO(8)^4} = e^1 + \tilde{U}e^2 + \tilde{S}e_2 - \left(\tilde{U}\tilde{S} - 1 - \tilde{U}^2\right)e_1 + W_I E_I . \quad (73)$$

Note that setting $\tilde{S} = 2i$ and $\tilde{U} = i$ reproduces the complex structure given in [5].

The lattice vectors orthogonal to $\Omega_{SO(8)^4}$ span the lattice $D_4^{\oplus 4}$. Using the expansion (46), their coefficients have to satisfy

$$-\left(\tilde{U}\tilde{S} - 1 - \tilde{U}^2\right)p^1 + p_1 - W_I^1 q_I + \tilde{S}p^2 + \tilde{U}(p_2 - W_I^2 q_I) = 0 . \quad (74)$$

As we know that these lattice vectors must be orthogonal to the complex structure for every value of \tilde{U} and \tilde{S} , we find the conditions

$$\begin{aligned} p^1 &= 0 & p_1 - W_I^1 q_I &= 0 \\ p^2 &= 0 & p_2 - W_I^2 q_I &= 0 . \end{aligned} \quad (75)$$

These equations are solved by the following four groups of lattice vectors:

	A	B	C	D
1	$E_7 - E_8$	$-E_{15} + E_{16}$	$-e_2 - E_1 + E_2$	$e_2 + E_9 - E_{10}$
2	$E_6 - E_7$	$-E_{14} + E_{15}$	$-E_2 + E_3$	$E_{10} - E_{11}$
3	$-e_1 - E_5 - E_6$	$e_1 + E_{13} + E_{14}$	$-E_3 + E_4$	$E_{11} - E_{12}$
4	$E_5 - E_6$	$-E_{13} + E_{14}$	$-E_3 - E_4$	$E_{11} + E_{12}$

(76)

It is not hard to see that there are no mutual intersections between the four groups, and that the intersections within each group are given by the D_4 matrix (67). This serves as an explicit check that (73) is indeed the correct holomorphic two-form of $K3$ at the $SO(8)^4$ point.

It should be clear that one can choose different linear combinations of the basis vectors in each block that still have the same inner product. This only means we can describe the positions of the D-branes by a different combination of cycles, which are of course linearly dependent on the cycles we have chosen before and span the same lattice.

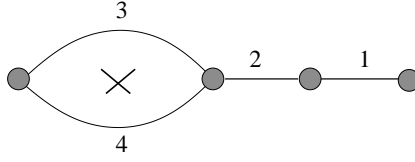


Figure 8: *The assignment between the geometrically constructed cycles between branes and the cycles of the table in the text. Note that the distribution of the cycles 1,3 and 4 is ambiguous.*

We can make an assignments between the cycles in the table and the cycles constructed geometrically as shown in Fig. 8.

When we are at the $SO(8)^4$ point, where 16 of the 20 cycles of $K3$ have shrunk, the only remaining degrees of freedom are the deformations of the remaining $T^2/Z_2 \times T^2$. The four cycles describing these deformations have to be orthogonal to all of the 16 brane cycles. There are four cycles satisfying this requirement,

$$\begin{array}{cc} e^1 + W_I^1 E_I & e^2 + W_I^2 E_I \\ e_1 & e_2 \end{array}, \quad (77)$$

and the torus cycles must be linear combinations of them. From the fibration perspective, the torus cycles are the cycles encircling two blocks (and thus two O-planes), so that the monodromy along the base part of those cycles is trivial. They can be either horizontal or vertical in the fibre, giving the four possibilities displayed in Fig. 9. Note that all of them have self-intersection zero and only those that wrap both fibre and base in different directions intersect twice.

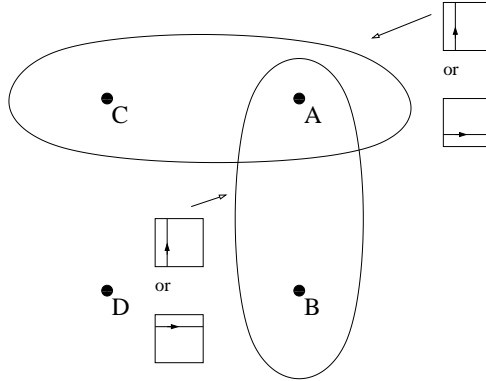


Figure 9: *The torus cycles have to encircle two blocks to ensure trivial monodromy along the basis part of the cycles. Note that the cycles which are orthogonal in the base and in the fibre intersect twice because of the orientation change introduced in going around the O-plane.*

To find out which linear combination of the forms in (77) gives which torus cycle, we will consider a point in moduli space where the gauge symmetry is enhanced from $SO(8)^4$ to $SO(16)^2$. At this point, there are 16 integral cycles orthogonal to Ω the intersection matrix of which is minus the Cartan matrix of $SO(16)^2$. Furthermore, we know that this situation corresponds to moving all D-branes onto two O7-planes. We will achieve

this leaving two of the four blocks untouched, while moving the D-branes from the other blocks onto them. This means that we blow up one of the cycles in each of the blocks that are moved, while collapsing two new cycles that sit in between the blocks. Doing this we find three independent linear combinations of the cycles in (77) that do not intersect any of the cycles that are shrunk.

Before explicitly performing this computation, we choose a new basis that is equivalent to (77):

$$\begin{aligned} \alpha &\equiv 2(e^1 + e_1 + W_I^1 E_I) & \beta &\equiv 2(e^2 + e_2 + W_I^2 E_I) \\ e_1 & & e_2 & . \end{aligned} \quad (78)$$

In this basis we can write Ω at the $SO(8)^4$ point as

$$\Omega_{SO(8)^4} = \frac{1}{2}(\alpha + Ue_2 + S\beta - USe_1) . \quad (79)$$

We also have switched to a new parameterization in terms of U and S . They will turn out to be the complex structures of the base and the fibre torus.

Let us now go to the $SO(16)^2$ point by setting $W_I^1 = 0$ in (71). After switching again from \tilde{S} and \tilde{U} to $S = \tilde{U}$ and $U/2 = \tilde{S} - \tilde{U}$, we find

$$\Omega_{SO(16)^2} = e^1 + \frac{U}{2}e_2 + \frac{S}{2}\beta - \frac{US}{2}e_1 . \quad (80)$$

The 16 integral cycles that are orthogonal to Ω are:

	E	F
1	$-e_2 - E_1 + E_2$	$e_2 + E_9 - E_{10}$
2	$-E_2 + E_3$	$E_{10} - E_{11}$
3	$-E_3 + E_4$	$E_{11} - E_{12}$
4	$-E_4 + E_5$	$E_{12} - E_{13}$
5	$-E_5 + E_6$	$E_{13} - E_{14}$
6	$-E_6 + E_7$	$E_{14} - E_{15}$
7	$-E_7 + E_8$	$E_{15} - E_{16}$
8	$E_7 + E_8$	$E_{15} + E_{16}$

(81)

They are labelled as shown in Fig. 10. Note that this means that we have moved block A onto block C and block B onto block D .

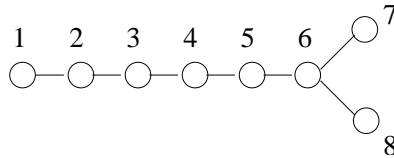


Figure 10: *The Dynkin diagram of $SO(16)$.*

One can check that, out of the basis displayed in (78), only α has a non-vanishing intersection with some of the 16 forms above, whereas all of them are orthogonal to

e_1, e_2, β . Thus, α is contained in the cycle that wraps the fibre in vertical direction and passes in between A, B and C, D (cf. Fig. 9). Furthermore, the non-zero intersection between e_1 and α tells us that e_1 wraps the fibre horizontally (for this argument we used $e_1 \cdot e_2 = e_1 \cdot \beta = 0$). Given these observations, it is natural to identify the four cycles (78) with the four cycles displayed in Fig. 9. More specifically, we now know that α is vertical in the fibre and passes in between A, B and C, D , while e_1 is horizontal in the fibre and passes in between A, C and B, D . The four cycles characterize the shape of $T^2/Z_2 \times T^2$. Other possible assignments between the cycles of (78) and those displayed in Fig. 9 correspond to reparameterizations of the tori and are therefore equivalent to our choice.

We now have to assign the cycles e_2 and β to the two remaining cycles of Fig. 9. For this purpose, we will explicitly construct the cycles Z_{XY} between the four $SO(8)$ blocks. Since they can be drawn in the same way as the cycles between the D-branes, cf. Fig. 11, we see that all of them must have self-intersection number -2 . We also know that their mutual intersections should be $Z_{XY} \cdot Z_{YZ} = 1$. From what we have learned so far, all of them should be either orthogonal to β and e_1 or orthogonal to e_2 and e_1 . It is easy to check that the first case is realized by:

$$\begin{aligned} Z_{AC} &= E_8 - E_1 - e_2 & Z_{AB} &= -(e_2 + e^2) - E_1 + E_8 - E_9 + E_{16} + e_1 \\ Z_{DB} &= E_{16} - E_9 - e_2 & Z_{CD} &= e_2 - e^2 . \end{aligned} \quad (82)$$

One can show that the second case is not possible. This can be seen from the following argument:

If we can find Z -cycles that are orthogonal to e_1 and e_2 , we can decompose them as

$$Z_{XY} = q_I E_I . \quad (83)$$

Note that the e_i are now responsible for making the Z -cycles wind around the base torus, so that we do not lose any generality by omitting them in the decomposition above. Because of the constraint $\sum q_I = 2\mathbb{Z}$, we can only have Z_{AB} intersecting one of the cycles in block A by putting $q_I = \pm \frac{1}{2}$ appropriately for $I = 5..8$. By the structure of the lattice, (46), this forces us to also set $q_I = \pm \frac{1}{2}$ for $I = 1..4$. It is clear that this will also make this cycle intersect with one of the cycles in block C , contradicting one of its defining properties. This means that we simply cannot construct the Z -cycles to be all orthogonal to e_1 and e_2 .

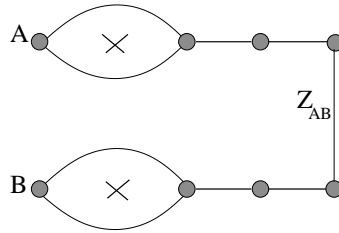


Figure 11: *The cycles connecting the blocks. Note that all cycles in this picture are built in the same way and thus all lie horizontally in the fibre.*

We can now use the intersections of the Z -cycles with the complex structure at the $SO(8)^4$ point, eq.(79), to measure their length and consistently distribute the four blocks

on the pillow. We find that

$$\begin{aligned}
Z_{AB} \cdot \Omega_{SO(8)^4} &= -U/2 & Z_{AC} \cdot \Omega_{SO(8)^4} &= -\frac{1}{2} \\
Z_{CD} \cdot \Omega_{SO(8)^4} &= -U/2 & Z_{DB} \cdot \Omega_{SO(8)^4} &= -\frac{1}{2} .
\end{aligned} \tag{84}$$

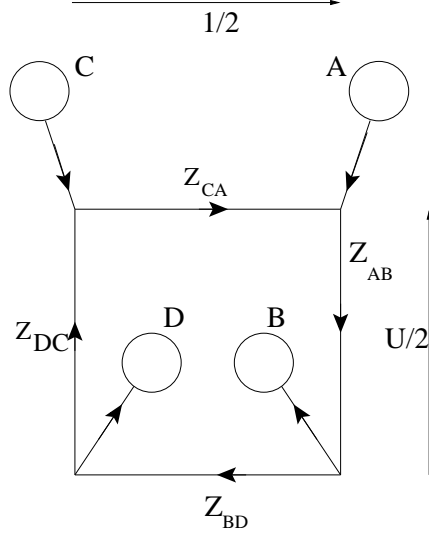


Figure 12: A schematic picture of the cycles between the blocks. We have drawn arrows to indicate the different orientations. Note that the Z -cycles have intersection $+1$ with the cycle they come from and -1 with the cycle they go to. Note that they sum up to a torus cycle, e_1 , telling us which blocks are encircled.

It is clear that we can add the two orthogonal cycles e_1 and β to the Z -cycles, $Z \rightarrow Z + ne_1 + m\beta$, without destroying their mutual intersection pattern. However, this changes their length by $n + Um$. This means that we can make the Z -cycles wind around the pillow n times in the real and m times in the imaginary direction. Calling the real direction of the base (fibre) x (x') and the imaginary direction of the base (fibre) y (y'), we can now make the identifications:

$$\begin{aligned}
e_1 &\text{ winds around } x \text{ and } x' \\
e_2 &\text{ winds around } x \text{ and } y' \\
\alpha &\text{ winds around } y \text{ and } y' \\
\beta &\text{ winds around } y \text{ and } x' .
\end{aligned} \tag{85}$$

Alternatively one can find the positions of e_2 and α by computing their intersections with the Z -cycles:

$$\begin{aligned}
e_2 \cdot Z_{CD} &= e_2 \cdot Z_{AB} = -1, & e_2 \cdot Z_{AC} &= e_2 \cdot Z_{DB} = 0, \\
\alpha \cdot Z_{AC} &= \alpha \cdot Z_{DB} = -1, & \alpha \cdot Z_{CD} &= \alpha \cdot Z_{AB} = 0 .
\end{aligned} \tag{86}$$

Note that these intersections change consistently when we let $Z \rightarrow Z + ne_1 + m\beta$. We display the distribution of the torus cycles in Fig. 13.

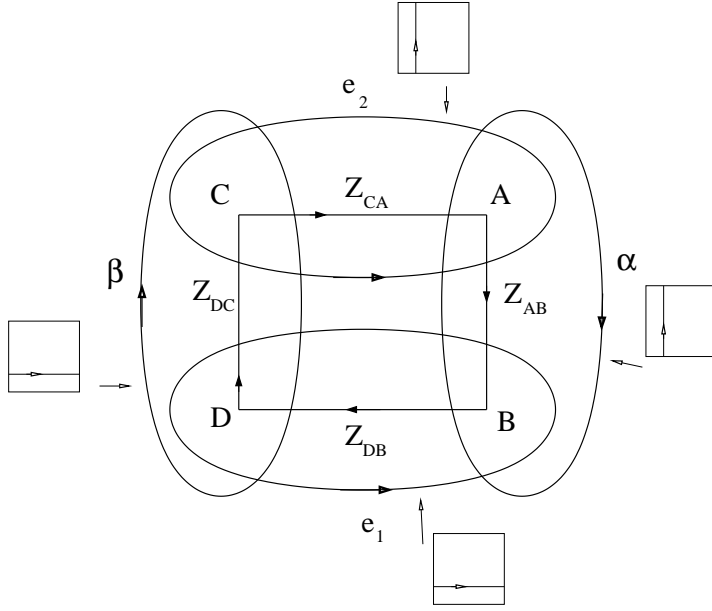


Figure 13: *The distribution of the torus cycles.*

At the orientifold point we can write the complex structure of $T^2/Z_2 \times T^2$ as

$$\begin{aligned}\Omega_{T^2/Z_2 \times T^2} &= (dx + Udy) \wedge (dx' + Sdy') \\ &= dx \wedge dx' + Sdx \wedge dy' + Udy \wedge dx' + SUdy \wedge dy' .\end{aligned}\quad (87)$$

In the above equation, U denotes the complex structure of the torus with unprimed coordinates, whereas S denotes the complex structure of the torus with primed coordinates. We have so far always switched freely between cycles and forms using the natural duality. We now make this identification explicit at the orientifold point:¹⁶

$$\begin{aligned}e_1 &= -2dy \wedge dy' \\ e_2 &= 2dy \wedge dx' \\ \alpha &= 2dx \wedge dx' \\ \beta &= 2dx \wedge dy' .\end{aligned}$$

Thus we have shown that the parameters U and S in

$$\Omega_{SO(8)^4} = \frac{1}{2} (\alpha + Ue_2 + S\beta - USe_1) , \quad (88)$$

do indeed describe the complex structure of the base and the fibre torus.

The findings of this section represent one consistent identification of the torus cycles and the Z -cycles that connect the four blocks. It is possible to add appropriate linear combinations of e_1 , e_2 , α and β without destroying the mutual intersections and the intersection pattern with the 16 cycles in the four $SO(8)$ blocks. What singles out our choice is the form of $\Omega_{SO(8)^4}$ in (73) as well as the $SO(16)$ that was implicitly defined in (80).

¹⁶ We have normalized the orientifold such that $\int_{T^2/Z_2} dx \wedge dy = 1/2$ and $\int_{T^2} \wedge dx' \wedge dy' = 1$.

9 D-Brane positions from periods and the weak coupling limit revisited

In this section, we study deformations away from the $SO(8)^4$ point. To achieve this, we have to rotate the complex structure such that not all of the vectors spanning the $D_4^{\oplus 4}$ lattice are orthogonal to it. In other words, we want to add terms proportional to the forms in (76) to $\Omega_{SO(8)^4}$. To do this, we switch to an orthogonal basis defined by

$$\begin{aligned}\tilde{E}_1 &= E_1 + e_2, & \tilde{E}_I &= E_I, & I &= 2..4, 10..12 \\ \tilde{E}_9 &= E_9 + e_2, & \tilde{E}_J &= E_J + e_1/2, & J &= 5..8, 13..16.\end{aligned}\quad (89)$$

As we will see, each \tilde{E}_I is responsible for moving only one of the D-branes when we rotate the complex structure to

$$\Omega = \frac{1}{2} \left(\alpha + Ue_2 + S\beta - (US - z^2) e_1 + 2\tilde{E}_I z_I \right). \quad (90)$$

Here z^2 denotes $z_I z_I$. Note that all of the \tilde{E}_I are orthogonal to $\Omega_{SO(8)^4}$, so that we only have to change the coefficient of e_1 to maintain the constraint $\Omega \cdot \Omega = 0$.

We can use the information about the length of the blown-up cycles to compute the new positions of the branes. Let e.g. $z_1 \neq 0$: This gives the first cycle of block C , $C_1 = -e_2 - E_1 + E_2$, the length $\Omega \cdot C_1 = z_1$, so that we move one brane away from the O-plane. As a result, the $SO(8)$ at block C is broken down to $SO(6)$. At the same time, the sizes of Z_{AC} and Z_{CD} are changed to

$$Z_{AC} \cdot \Omega = -\frac{1}{2} + z_1, \quad Z_{CD} \cdot \Omega = -\frac{U}{2} - z_1. \quad (91)$$

Thus we can move the brane from block C onto block A by choosing $z_1 = \frac{1}{2}$, or onto block D by choosing $z_1 = -U/2$. This can also be seen from the overall gauge group which is $SO(6) \times SO(10) \times SO(8)^2$ for these two values of z_1 .

As we have seen in the last paragraph, z_1 controls the position of one of the four D-branes located at block C , as compared to the position of the O-plane at block C . If we let all of the z_I be non-zero, we find the following values for the lengths of the cycles in block C :

$$\begin{array}{c|c} C_I & C_I \cdot \Omega \\ \hline C_1 & z_1 - z_2 \\ C_2 & z_2 - z_3 \\ C_3 & z_3 - z_4 \\ C_4 & z_3 + z_4 \end{array} \quad (92)$$

To determine the D-brane positions, it is important to note that the D-branes are moving on a pillow, T^2/Z_2 . We thus use a local coordinate system equivalent to \mathbb{C}/Z_2 . It is centered at the position of the O-plane of block C at one of the corners of the pillow. The intersections of the cycles with Ω are line integrals along the base part of the cycles C_I (see Fig. 14), multiplied by the line integral of their fibre part (which can be set to

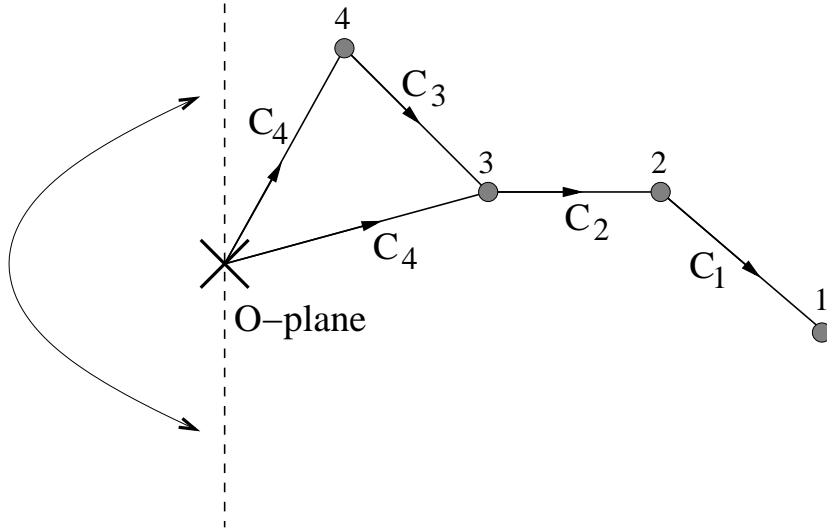


Figure 14: *The positions of D-branes on \mathbb{C}/Z_2 are measured by complex line integrals along the cycles C_I . As indicated in the picture, \mathbb{C}/Z_2 is obtained from the complex plane by gluing the upper part of the dashed line to its lower part. Due to the presence of the O-plane, the line integral along C_4 has to be evaluated as indicated by the arrows. Using (92), one can see that the positions of the branes are given by the z_I .*

unity locally). This is of importance for the length of C_4 : due to the orientation flip in the fibre when surrounding the O-plane, we have to evaluate both parts of the line integral going from the O-plane to the D-branes to account for the extra minus sign. This is indicated by the arrows that are attached to the cycles in Fig. 14. It is then easy to see that associating the z_I with the positions of the D-branes yields the correct results. Note that one achieves the same gauge enhancement for $z_3 = z_4$ and $z_3 = -z_4$, because for both values one of the C_I is collapsed, cf. (92). Thus the D-branes labelled 3 and 4 have to be at the same position in both cases, which fits with the fact that $z_I = -z_I$ holds due to the Z_2 action.

By the same reasoning, the remaining z_I give the positions of the other D-branes measured relative to the respective O-plane. For example, the moduli z_5 to z_8 give the positions of the D-branes of block A (see (76)). We have also shown that we can connect the four blocks by following the gauge enhancement that arises when we move a brane from one block to another, cf. (91). This means that we can also easily connect the four coordinate systems that are present at the position of each O-plane. We have now achieved our goal of explicitly mapping the holomorphic 2-form Ω to the positions of the D-branes. For this we have used forms dual to integral cycles. These are the cycles that support the M-theory flux which can be used to stabilize the D-branes. By using our results, it is possible to derive the positions of the D-branes from a given complex structure (unless the solution is driven away from the weak coupling limit). We thus view this work as an important step towards the explicit positioning of D-branes by M-theory flux.

The geometric constructions of this article only make sense in the weak coupling limit, in which the monodromies of the branes of F-theory are restricted to those of D7-branes and O7-planes. It is crucial that the positions of the D-branes and the shape of

the base torus factorize in the weak coupling limit, $S \rightarrow i\infty$. The shape of the base torus is measured by multiplying the cycles α , β , e_1 and e_2 with Ω . The result is independent of the positions of the branes in the weak coupling limit, as the only potential source of interference is the z^2 in $\alpha \cdot \Omega = US - z^2$, which is negligible as compared to US . Thus the branes can really be treated as moving on T_2/Z_2 without backreaction in the weak coupling limit.

Certain gauge groups, although present in F-theory, do not show up in perturbative type IIB orientifolds and thus cannot be seen in the weak coupling limit. The lattice of forms orthogonal to Ω only has the structure of gauge groups known from type IIB orientifold models when we let $S \rightarrow i\infty$ in (71). This comes about as follows: Starting from the $SO(8)^4$ point, we can cancel all terms proportional to $W_I E_I$ in (71) when we are at finite coupling. In the limit $S \rightarrow i\infty$, the fact that β has S as its prefactor prevents the cancellation of the term $W_I^2 E_I$ in Ω . The presence of this term ensures that only perturbatively known gauge enhancements arise.

10 Summary and Outlook

Our main points in this article were the implications of the weak coupling limit (which is necessary if one wants to talk about D7-branes moving in a background Calabi-Yau orientifold) and the description of D7-brane motion on \mathbb{CP}^1 in terms of integral M-theory cycles.

Regarding the weak coupling limit, we have rederived the fact that the deficit angle of a D7-brane is zero in a domain whose size is controlled by the coupling. Furthermore, we have pointed out ‘physics obstructions’ that arise in the weak coupling limit: The polynomial that describes the D7-brane has to take a special form in the weak coupling limit, so that some degrees of freedom are obstructed. We have counted the relevant degrees of freedom explicitly for F-theory on elliptically fibred spaces with base $\mathbb{CP}^1 \times \mathbb{CP}^1$ (which is dual to the Bianchi-Sagnotti-Gimon-Polchinski model) and with base \mathbb{CP}^2 . From a local perspective, the obstructions arise at intersections between D7-branes and O7-planes. They demand that D7-branes always intersect O7-planes in double-intersection-points (in the fundamental domain of the orientifold model; not in the double-cover Calabi-Yau, where this would be a trivial statement). The obstructions imply that a D7-brane intersecting an O7-plane has fewer degrees of freedom than a corresponding holomorphic submanifold. It would be very interesting to analyse the implications of this effect explicitly in higher-dimensional models.

The rest of this paper was devoted to an explicit discussion of the degrees of freedom of F-theory on $K3$, corresponding to type IIB string theory compactified on an orientifold of T^2 . We were able to construct and visualize the cycles that control the motion of D7-branes on the base. Using these cycles, we have achieved a mapping between the positions of the D-branes and the values of the complex structure moduli. This was done using the singularities that arise at special points in the moduli space.

We consider our analysis an important preliminary step for the study of more realistic D7-brane models. First, realistic models should contain fluxes to stabilize the geometry and the D7-brane positions. Using a higher-dimensional generalization of our map between cycles and D7-brane positions, it should be possible to determine explicitly the flux

stabilizing a desired D7-brane configuration. A first step in this direction, from which one should gain valuable intuition, might be the reconsideration of F-theory on $K3 \times K3$ with our tools. Second, we want to consider F-theory compactifications on elliptically fibred Calabi-Yau manifolds of higher dimension. We expect new kinds of cycles and new configurations, for example cycles describing the recombination of D7-branes and configurations leading to gauge groups that are not simply laced.

When F-theory is compactified on a six-dimensional manifold, the latter can be analysed with the methods used in this paper. The recombination of two intersecting D7-branes can be locally described as a deformation of the conifold, so that an S^3 emerges. This S^3 can be seen as the combination of a disc spanned in the tunnel connecting the two D7-branes and a horizontal cycle in the fibre torus.

Although there exists a rich literature on elliptically fibred Calabi-Yau manifolds (see e.g. [39, 40, 45–49]), the direct visualization of the geometric objects achieved in this paper becomes harder in higher dimensions. We hope that the use of toric geometry methods will allow for a geometric understanding and simple combinatorial analysis in such cases.

Acknowledgments

We would like to thank Tae-Won Ha, Christoph Lüdeling, Dieter Lüst, Michele Trapletti, and Roberto Valandro for useful comments and discussions.

References

- [1] S. B. Giddings, S. Kachru and J. Polchinski, “Hierarchies from fluxes in string compactifications,” *Phys. Rev. D* **66** 106006 (2002) [arXiv:hep-th/0105097];
S. Kachru, R. Kallosh, A. Linde and S. P. Trivedi, “De Sitter vacua in string theory,” *Phys. Rev. D* **68**, 046005 (2003) [arXiv:hep-th/0301240].
- [2] K. Becker and M. Becker, “M-theory on Eight-Manifolds,” *Nucl. Phys. B* **477**, 155 (1996) [arXiv:hep-th/9605053].
- [3] S. Gukov, C. Vafa and E. Witten, “CFT’s from Calabi-Yau four-folds,” *Nucl. Phys. B* **584**, 69 (2000) [Erratum-ibid. *B* **608**, 477 (2001)] [arXiv:hep-th/9906070].
- [4] K. Dasgupta, G. Rajesh and S. Sethi, “M theory, orientifolds and G-flux,” *JHEP* **9908** (1999) 023 [arXiv:hep-th/9908088].
- [5] L. Gorlich, S. Kachru, P. K. Tripathy and S. P. Trivedi, “Gaugino condensation and nonperturbative superpotentials in flux compactifications,” *JHEP* **0412**, 074 (2004) [arXiv:hep-th/0407130].
- [6] D. Lüst, P. Mayr, S. Reffert and S. Stieberger, “F-theory flux, destabilization of orientifolds and soft terms on D7-branes,” *Nucl. Phys. B* **732**, 243 (2006) [arXiv:hep-th/0501139].

- [7] H. Jockers and J. Louis, “The effective action of D7-branes in $N = 1$ Calabi-Yau orientifolds,” Nucl. Phys. B **705**, 167 (2005) [arXiv:hep-th/0409098].
- [8] H. Jockers and J. Louis, “D-terms and F-terms from D7-brane fluxes,” Nucl. Phys. B **718**, 203 (2005) [arXiv:hep-th/0502059].
- [9] J. Gomis, F. Marchesano and D. Mateos, “An open string landscape,” JHEP **0511**, 021 (2005) [arXiv:hep-th/0506179].
- [10] T. Watari and T. Yanagida, “Product-group unification in type IIB string theory,” Phys. Rev. D **70**, 036009 (2004) [arXiv:hep-ph/0402160].
- [11] C. Vafa, “Evidence for F-theory,” Nucl. Phys. B **469**, 403 (1996) [arXiv:hep-th/9602022].
- [12] P. S. Aspinwall and R. Kallosh, “Fixing all moduli for M-theory on $K3 \times K3$,” JHEP **0510** (2005) 001 [arXiv:hep-th/0506014].
- [13] A. Sen, “Orientifold limit of F-theory vacua,” Phys. Rev. D **55**, 7345 (1997) [arXiv:hep-th/9702165].
- [14] J. F. G. Cascales, M. P. Garcia del Moral, F. Quevedo and A. M. Uranga, “Realistic D-brane models on warped throats: Fluxes, hierarchies and moduli stabilization,” JHEP **0402** (2004) 031 [arXiv:hep-th/0312051].
- [15] H. Verlinde and M. Wijnholt, “Building the standard model on a D3-brane,” JHEP **0701** (2007) 106 [arXiv:hep-th/0508089].
- [16] B. R. Greene, A. D. Shapere, C. Vafa and S. T. Yau, “Stringy Cosmic Strings And Noncompact Calabi-Yau Manifolds,” Nucl. Phys. B **337**, 1 (1990).
- [17] G. W. Gibbons, M. B. Green and M. J. Perry, “Instantons and Seven-Branes in Type IIB Superstring Theory,” Phys. Lett. B **370**, 37 (1996) [arXiv:hep-th/9511080].
- [18] E. A. Bergshoeff, J. Hartong, T. Ortin and D. Roest, “Seven-branes and supersymmetry,” JHEP **0702**, 003 (2007) [arXiv:hep-th/0612072].
- [19] M. Bianchi and A. Sagnotti, “Open Strings and the Relative Modular Group,” Phys. Lett. B **231**, 389 (1989).
- [20] E. G. Gimon and J. Polchinski, “Consistency Conditions for Orientifolds and D-Manifolds,” Phys. Rev. D **54**, 1667 (1996) [arXiv:hep-th/9601038].
- [21] W. Lerche, P. Mayr and N. Warner, “Holomorphic $N = 1$ special geometry of open-closed type II strings,” arXiv:hep-th/0207259.
- [22] W. Lerche, P. Mayr and N. Warner, “ $N = 1$ special geometry, mixed Hodge variations and toric geometry,” arXiv:hep-th/0208039.
- [23] W. Lerche, “Special geometry and mirror symmetry for open string backgrounds with $N = 1$ supersymmetry,” arXiv:hep-th/0312326.
- [24] A. Sen, “F-theory and Orientifolds,” Nucl. Phys. B **475**, 562 (1996) [arXiv:hep-th/9605150].

- [25] W. Lerche, “On the heterotic/F-theory duality in eight dimensions,” arXiv:hep-th/9910207.
- [26] C. V. Johnson, “D-brane primer,” arXiv:hep-th/0007170.
- [27] K. Chandrasekharan, “Elliptic Functions,” *Berlin, Germany: Springer Verlag (1985) 189 p*
- [28] A. Sen, “F-theory and the Gimon-Polchinski orientifold,” Nucl. Phys. B **498**, 135 (1997) [arXiv:hep-th/9702061].
- [29] T. Hübsch, “Calabi-Yau manifolds: A Bestiary for physicists,” *Singapore, Singapore: World Scientific (1992) 362 p*.
- [30] P. Griffiths and J. Harris, ”Principles of Algebraic Geometry”; John Wiley & Sons, Inc. (1978) (USA).
- [31] Kunihiko Kodaira, “A Theorem of Completeness of Characteristic Systems for Analytic Families of Compact Submanifolds of Complex Manifolds,” Annals of Mathematics, 75(1), 146-162, 1962 MR 24:A3665b
- [32] I. Brunner, M. R. Douglas, A. E. Lawrence and C. Romelsberger, JHEP **0008** (2000) 015 [arXiv:hep-th/9906200].
- [33] P. S. Aspinwall, “K3 surfaces and string duality,” arXiv:hep-th/9611137.
- [34] J. Polchinski, “String theory. Vol. 2: Superstring theory and beyond,” *Cambridge, UK: Univ. Pr. (1998) 531 p*.
- [35] P. Candelas, P. S. Green and T. Hübsch, “Rolling Among Calabi-Yau Vacua,” Nucl. Phys. B **330**, 49 (1990).
- [36] D. R. Morrison and C. Vafa, “Compactifications of F-theory on Calabi–Yau Threefolds – I,” Nucl. Phys. B **473**, 74 (1996) [arXiv:hep-th/9602114];
D. R. Morrison and C. Vafa, “Compactifications of F-theory on Calabi–Yau Threefolds – II,” Nucl. Phys. B **476**, 437 (1996) [arXiv:hep-th/9603161].
- [37] P. S. Aspinwall, “Enhanced Gauge Symmetries and Calabi-Yau Threefolds,” Phys. Lett. B **371**, 231 (1996) [arXiv:hep-th/9511171].
- [38] P. S. Aspinwall and M. Gross, “The SO(32) Heterotic String on a K3 Surface,” Phys. Lett. B **387**, 735 (1996) [arXiv:hep-th/9605131].
- [39] P. S. Aspinwall, S. H. Katz and D. R. Morrison, “Lie groups, Calabi-Yau threefolds, and F-theory,” Adv. Theor. Math. Phys. **4**, 95 (2000) [arXiv:hep-th/0002012].
- [40] M. Bershadsky, K. A. Intriligator, S. Kachru, D. R. Morrison, V. Sadov and C. Vafa, “Geometric singularities and enhanced gauge symmetries,” Nucl. Phys. B **481**, 215 (1996) [arXiv:hep-th/9605200].
- [41] E. Witten, “String theory dynamics in various dimensions,” Nucl. Phys. B **443**, 85 (1995) [arXiv:hep-th/9503124].
- [42] C. Vafa, “Lectures on strings and dualities,” arXiv:hep-th/9702201.

- [43] G. Lopes Cardoso, G. Curio, D. Lust and T. Mohaupt, “On the duality between the heterotic string and F-theory in 8 dimensions,” *Phys. Lett. B* **389** (1996) 479 [arXiv:hep-th/9609111].
- [44] W. Lerche and S. Stieberger, “Prepotential, mirror map and F-theory on K3,” *Adv. Theor. Math. Phys.* **2**, 1105 (1998) [Erratum-ibid. **3**, 1199 (1999)] [arXiv:hep-th/9804176].
- [45] V. V. Batyrev, “Dual polyhedra and mirror symmetry for Calabi-Yau hypersurfaces in toric varieties,” *J. Alg. Geom.* **3**, 493 (1994).
- [46] A. Klemm, B. Lian, S. S. Roan and S. T. Yau, “Calabi-Yau fourfolds for M- and F-theory compactifications,” *Nucl. Phys. B* **518**, 515 (1998) [arXiv:hep-th/9701023].
- [47] P. Candelas and A. Font, “Duality between the webs of heterotic and type II vacua,” *Nucl. Phys. B* **511** (1998) 295 [arXiv:hep-th/9603170].
- [48] E. Perevalov and H. Skarke, “Enhanced gauge symmetry in type II and F-theory compactifications: Dynkin diagrams from polyhedra,” *Nucl. Phys. B* **505** (1997) 679 [arXiv:hep-th/9704129].
- [49] P. Candelas, E. Perevalov and G. Rajesh, “Toric geometry and enhanced gauge symmetry of F-theory/heterotic vacua,” *Nucl. Phys. B* **507** (1997) 445 [arXiv:hep-th/9704097].